Change Detection for Surface Mining Boundary Based on Multi-source Remote
Sensing Images

KAWIPA SUKKEE

A THESIS SUBMITTED IN PARTIAL FULFILLMENT OF
THE REQUIREMENTS FOR THE MASTER DEGREE OF SCIENCE
IN GEOINFORMATICS
FACULTY OF GEOINFORMATICS
BURAPHA UNIVERSITY
2022
COPYRIGHT OF BURAPHA UNIVERSITY

การตรวจสอบการเปลี่ยนแปลงของขอบเขตการทำเหมืองแร่แบบเปิด โดยการประยุกต์ใช้
แหล่งข้อมูลจากการสำรวจระยะไกล

กวิภา สุขขี

Change Detection for Surface Mining Boundary Based on Multi-source Remote
Sensing Images

KAWIPA SUKKEE

A THESIS SUBMITTED IN PARTIAL FULFILLMENT OF
THE REQUIREMENTS FOR THE MASTER DEGREE OF SCIENCE
IN GEOINFORMATICS
FACULTY OF GEOINFORMATICS
BURAPHA UNIVERSITY
2022

The Thesis of Kawipa Sukkee has been approved by the examining committee to be partial fulfillment of the requirements for the Master Degree of Science in Geoinformatics of Burapha University

Advisory Committee   Examining Committee

Principal advisor

.... Principal
                                                                        examiner
(Professor Zhenfeng Shao)   (Professor Li Tao)

                                              .... Member
Co-advisor   (Professor Zhenfeng Shao)

.... Member
(Dr. Kitsanai Charoenjit)   (Dr. Kitsanai Charoenjit)

                                              .... Member
                                       (Professor Hong Shu)

.... Dean of the Faculty of Geoinformatics
    (Dr. Kitsanai Charoenjit)

....

        This Thesis has been approved by Graduate School Burapha University to be partial fulfillment of the requirements for the Master Degree of Science in Geoinformatics of Burapha University

.... Dean of Graduate School
    (Associate Professor Dr. Nujjaree Chaimongkol)

....

63910060:   MAJOR: GEOINFORMATICS; M.Sc. (GEOINFORMATICS)

KEYWORDS: Remote Sensing, InSAR, Random Forest Algorithm, Digital Elevation Model, Surface Mining

KAWIPA SUKKEE : CHANGE DETECTION FOR SURFACE MINING BOUNDARY BASED ON MULTI-SOURCE REMOTE SENSING IMAGES. ADVISORY COMMITTEE: ZHENFENG SHAO, Ph.D., KITSANAI CHAROENJIT, Ph.D., 2022.

Mining is an important industry in Thailand. It can levy gross mineral royalties an average of 3 billion Thai baht per year, and The Minerals Act, B.E. 2560, regulates the industry. The Department of Primary Industries and Mines (DPIM), part of the Ministry of Industry, is in charge of monitoring and promoting the mining industry, including mineral trading, as well as establishing safety and pollution-control regulations. In the past, mining outside the permissible limits frequently occurred. It negatively affects royalty storage and the environment. Because of mining supervision, there are also limitations to tools, methods, personnel, expenses, as well as regulatory frequency.

This study applied data from freely available satellite data and open-source software. To assess the suitability of satellite technology applications to detect changes in horizontal and vertical mining in small mining areas to suit mining areas in Thailand. There are two study areas, selected from the average size of all mines currently mining. The satellite data used in this study include Sentinel-1, Sentinel-2, and Landsat 8. The validating data is from the allowed agent to ensure the reliability and accuracy comprising topographical mining data measured by unmanned aircraft (UAV) from DPIM which have high resolution, and the Digital Elevation Model (DEM) from the Royal Thai Survey Department (RTSD).

The research methodology used in this study is to extract the boundary of horizontal mining by applying Sentinel-2 data and Landsat 8 by Mean-Shift algorithm and classifying mining areas with Random Forest (RF) algorithms obtains classified into two classes: Mining and Non-mining. The performance of the classification result was assessed based on the confusion matrix formed using the 32 observations for study area 1 and 34 observations for study area 2 from the test samples. The overall

accuracy was calculated using the confusion matrix. The vertical boundary mining analysis has applied Sentinel-1 data to extract DEM using InSAR techniques. Then used the DEM compared with RTSD DEM, statistically analyzed by using a coefficient of determination (R^2) and root mean squared error (RMSE). Analyzing changes in vertical mining using DEM data obtained from the InSAR technique and analyzing the volume changes of two periods.

The result of horizontal mining boundary extraction from Sentinel-2 and Landsat 8, In the first study area round 1 has an overall accuracy of 95.66% and 86.57%. Round 2 of the first study area is 97.47% and 96.50%. In the second study area, round 1, the overall accuracy is 100% and 99.35%. Round 2 of the second study area is 99.26% and 95.90% respectively. Based on validation results, the satellite data from Sentinel-2 is more accurate than the horizontal boundary of mining compared to Landsat 8 data. When using the horizontal boundary of mining from sentinel-2 data to analyze changes in horizontal mining areas, the data of the mining area was used to analyze the changes in the horizontal mining area. In study area 1, mining expansion was 11.64% of the original mining area, according to the reference. And in study area 2, mining expansion was 11.79% of the original mining area, according to the reference. The result of DEM extraction has obtained the result as 14 m resolution of DEM and correlates when compares to DEM from UAV. The result found that the R^2 and RMSE values are 0.6038 and 34.279 for the study area 1 of the first round, 0.5621 and 35.731 for study area 1 of the second round, 0.2947 and 55.704 for study area 2 of the first round, and 0.2666 and 57.603 for the study area 1 of the second round. However, the DEM extracted from the Sentinel-1 is highly accurate, but it is not enough to need of vertical mining change analysis of a small mining area.

Finally, the application and method of this research to use in change detection of horizontal and vertical surface mining boundaries. Sentinel-2 has a medium level of suitability for change detection of horizontal mining boundary since the change characteristic is similar to the reference data. Landsat-8 is not a suitable choice for horizontal change detection in small area mining and Sentinel-1 is not suitable for detecting the change in vertical mining in the small mining areas.

ACKNOWLEDGEMENTS

TABLE OF CONTENTS

Page

List of tables

List of figures

LIST OF ABBREVIATIONS

DEM	Digital Elevation Model
DPIM	Department of Primary Industries and Mines
cm	Centimeter
InSAR	Interferometric Synthetic Aperture Radar
m	Meter
m^2	Square meter
m^3	Cubic meter
OTB	Orfeo Toolbox
QGIS	Quantum Geographic Information System
R^2	Coefficient of Determination
RF	Random Forest Algorithm
RMSE	Root Mean Squared Error
RTSD	Royal Thai Survey Department
SAR	Synthetic Aperture Radar
SCP	Semi-Automatic Classification Plugin
SNAP	Sentinel Application Platform
sq.km.	Square kilometers
UAV	Unmanned Aircraft vehicles
%	Percent

CHAPTER 1
INTRODUCTION

Mining is an important industry in Thailand. On December 22th, 2020, there were 927 mining concessions with the Department of Primary Industries and Mines (DPIM), being the main government authority and responsible for regulating and promoting mining in Thailand. Mining can be classified into two classes comprise underground and surface mining. Most of the mines in Thailand are surface mining, also known as opencast mining or open-pit mining, which refers to the method of extracting minerals from the earth by their removal from an open pit [1]. The DPIM has manipulated mining operations to get more efficient in responding to the demand for industrial materials. Also, it has the duty of maintaining the operation to be legal, regulated, and eco-friendly under the minerals act, B.E. 2560 [2]. The monitoring starts at the request of mining permission till the restoration of the used mines. Nowadays, the DPIM has a spatial investigation of various purposes of mining such as, mining operation followed by authorized layout, change of mining operation investigation, mineral storage investigation, and mining boundary investigation. It is important to operate the mining process in an authorized boundary. There are many disputed cases of unauthorized mining, due to the illegal mining area expanding. Essential evidences of unauthorized mining are mining boundary surveying reports, reports of volume and value of minerals, damages reports, etc. While each of the mentioned case has millions THB damaged values, the surveyed data is the primary data for estimating the damaged values

Mining geographical data is essential in field surveying management, which is acquired from field measurement and remote sensing. The field measurement could be done by total station instrument. The remote sensing could be achieved by a terrestrial laser scanner or by Unmanned Aerial vehicles (UAV). These data acquirements are regularly done through time and are precisely achieved, such as aerial photos and digital elevation models (DEM) which are widely used nowadays. The photos taken by the UAVs are processed through orthorectification to correct relief displacement, resulting in high-accuracy orthophotos and DEM stored in raster

form. The DEM fetched from the UAV is similarly processed with orthophotos. There is also an official DEM from the Royal Thai survey department (RTSD) which is the government's primary agent for producing DEM.

DPIM has applied remote sensing technology from UAV together with GNSS satellite technology for surveying, resulting in orthophotos and DEM which can be accurately used to check the horizontal and vertical mining boundary and can be accepted in government agencies and related agencies. Yet, it needs plenty of surveying time as well as the prevention of errors in the products is not as good as it should be. Therefore, having data in more frequent intervals and covering more areas will reduce errors and increase work efficiency. Applying satellite data to solve such problems is a good choice. Satellite technology in remote sensing technologies has been widely used in mining-related applications such as mapping of the surface mineralogy, topography, and land cover. Those basic data are quite important to monitor and regulate legal mining.

In mining field, several research have made use of satellite data and remote sensing techniques to extract and detect changes in mining areas, i.e. Multispectral images were used to delineate open-pit mining boundaries, Sentenel-2 data is being used to extract the boundary, Orfeo Toolbox (OTB) was used for digital processing of imageries, Mean-Shift segmentation algorithm and Random forest algorithm are used for extraction horizontal mining boundary [3]. InSAR coherence has been used to evaluate the feasibility of detecting illegal surface mining process by Sentinel-1data. The results show that InSAR coherence is suitable for identifying mining activities [4]. Small-scale surface mining of gold placers such as Detection, mapping, and temporal analysis through the use of free Sentinel-2 satellite imagery was utilized to identify mining areas and to understand the dynamics in landcover [5]. Many studies focused on either there were horizontal or vertical changes in mines, but the changes of mines literally occurred in both directions. The one-dimension inspection could not effectively prevent illegal expansion of mining. There was also a study about combining TanDEM-X and SRTM DEMs and spectral images to improve the detection of large open excavation areas using multi-temporal DEM and multispectral satellite imagery, object-based image analysis, and RF algorithms. The results show that this method can be applied to larger areas [6]. However, most of the mines in

Thailand are small and these satellite images and processing techniques have not been applied to detect mining changes.

Although the traditional methods of surveying have obtained detailed data that has high accuracy, but they need a lot of time, personnel, and operating costs. These conditions lead to struggling in performing inspections in a short time when compared to satellite technology. The cyclic observations by the satellite technology allow periodic updates of data from the surface mining. This allows monitoring of changes in land cover over time. Measurements from remote sensing technology are unlike field-based data collection [7], since they can reduce time, expenses and personnel in operation

This study aims to use the freely available satellite imagery including Sentinel-1, Sentinel-2 and Landsat-8 and open-source software to detect the changes in the horizontal and the vertical boundary of surface mining at the small-scale mining area. Two mining areas in Thailand were selected based on average size of all mining area throughout the country. The InSAR techniques were used to extract a DEM from Sentinel-1 data by SNAP software and calibration by RTSD DEM. The Mean-Shift segmentation algorithm and RF algorithm were used for extracting horizontal mining boundaries from Sentinel-2 and Landsat 8 imagery. After getting both results of horizontal and vertical boundaries, I analyzed the area changes by matching it based on the same source. I used the change area data as a base in the comparison process to determine the accuracy of the data that has been processed. The high accurate data was obtained from UAVs. The statistic approach for validation consists of R^2 and RMSE. Finally, I determined a guideline for selecting the best and the most suitable data for mining boundary monitoring. Mining boundary can be investigated before operating the fieldwork, and satellite technology will be more effective in mining investigation.

1.1 Research Question

1.1.1 How is the accuracy of extracting mining boundary from Sentinel-2 and Landsat 8 satellite images and detecting changes in horizontal mining boundary?

1.1.2 How is the accuracy of DEM extraction from Sentinel-1 data using InSAR techniques and detecting changes in vertical mining boundary?

1.1.3 How efficient of the satellite technology in this study appropriate in its application to detect changes in horizontal and vertical mining in small mining areas?

1.2 Objectives

The principal objectives of the research are to apply multi-source satellite imagery for change detection of small surface mining boundary, and to focus on open-source software in processing. The specific objectives of this thesis are:

1.2.1 To assess the change detection performance of the horizontal mining boundary from Sentinel-2 and Landsat 8 data.

1.2.2 To assess the effectiveness of using the DEM generated by InSAR techniques from Sentinel-1 data to detect changes in the vertical mining boundary.

1.2.3 To assess the suitability of using the satellite technology to detect changes in horizontal and vertical mining in small mining areas.

1.3 The main contents of this dissertation

The main contents of this dissertation are:

1.3.1 Extracting surface mining boundary from multi-source satellite imagery using RF algorithm then detecting mining changes and comparing them to open-mining changes from UAV data.

1.3.2 Generating a DEM from SAR satellites using an InSAR technique then detecting mining changes and finally, comparing the results with a DEM generated from UAV data.

1.3.3 Detecting changes in mining boundary and determining the guidelines for the use of satellite technology in the change detection of surface mining boundary from different remotely sensed datasets.

1.4 Study Area

Two mining areas in Saraburi and Lopburi Province in Thailand were selected based on average size of all mining area throughout the country. Each study area is described as follow:

1.4.1 Study area 1 is a calcite mining area of Surint Omya Chemicals (Thailand) Co.,Ltd., located in Lopburi Province, with a mining permit of 271,395.893 m² as shown in Figure 1. This study area is characterized by flat terrain and the mean elevation of the surrounding area is about 73 m (msl). The elevation of the mining area based on the reference of round 1 mining is 106 m and the minimum elevation is -25 m.

1.4.2 Study area 2 is an industrial stone area for the construction industry of Silasanon Co., Ltd., located in Saraburi Province, with an area of 410,008.780 m² as show in Figure 2. This mining area is characterized by mountainous slope mining. The average pre-mining elevation is 171m, with a maximum of 292 m and a minimum of 83 m. After mining has an elevation of the mining area based on the reference of round 1 mining, the maximum is 246 m and the minimum is 55 m.

Figure 1 Study area 1
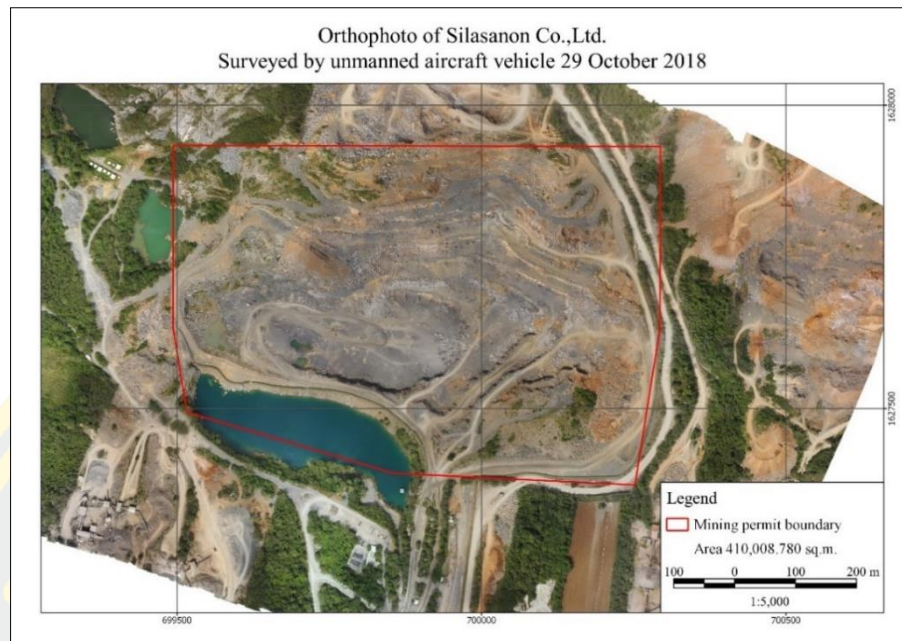
Figure 2 Study area 2

1.5 The structure of this dissertation

This thesis is separated into five chapters. Chapter 1 presents the mining in Thailand, the general background of the study, the research question, the objectives, the main contents of this dissertation, and the study area. Chapter 2 contains a literature review of remote sensing, UAV, InSAR, and in relation to earlier research. In Chapter 3 will outline the data used, the technique, and the overall study process the experiment results are presented in Chapter 4, boundary Extraction, DEM extraction and calibration, and change detection. Finally, Chapter 5 is a dissertation summary, offering broad conclusions and recommendations for further research in this area. The thesis structure is shown in Figure 3.
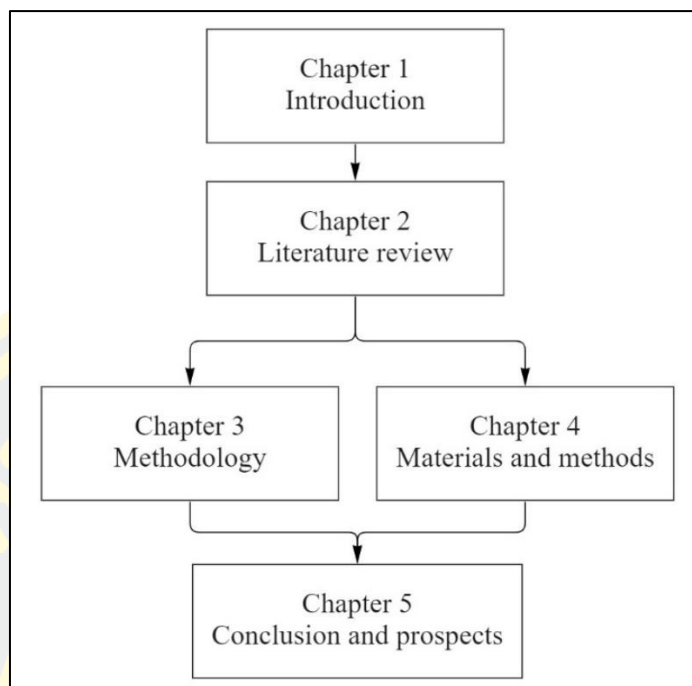
Figure 3 The relationship diagram of the dissertation

CHAPTER 2
LITERATURE REVIEW

The propose in this chapter is to provide a general review consisting of 5 sections including Mining in Thailand, remote sensing, UAV, InSAR techniques, and research review.

2.1 Mining in Thailand

Thailand has benefited from the mineral mining industry for a long time ago. There are essential metallic minerals such as tin, tungsten, niobium, tantalum, lead, zinc, gold, iron, and stibnite. Also, the non-metallic minerals such as feldspar, clay minerals, fluorite, barite, potash, and rock salt play an essential role in Thailand's industry. The importance of rocks and dimension stones as essential materials for industry and building is growing [8]. Thailand's mining industry has continued to thrive as a result of escalating the demand from both domestic and foreign trading [9]. The Minerals Act, B.E. 2560 (A.D. 2017) [2], which went into effect on August 29, 2019, regulates mining in Thailand. The Minerals Act of B.E. 2560 (A.D. 2017) replaced the Minerals Act of B.E. 2510 (A.D. 1967) and merged the previous Minerals Act and the Mineral Royalty Act into a single piece of law. The Ministry of Industry's Department of Primary Industries and Mines (DPIM) is in charge of overseeing and promoting the mining industry, including mineral commerce, as well as establishing safety and pollution-control regulations. Prospecting and exploration, mining, mineral processing and metallurgical processing, mineral possession, transportation and mining tax, procurement, trading, and storage of minerals, and foreign minerals trading are the six types of mining applications based on their operational stage. Mineral royalty tariffs must be spent by the companies. The mineral royalty tariff is a type of tax that the state collects from mining enterprises. The minerals royalty tariff rates are determined by the price of the metal in the individual ores. According to the Minerals Act and the Ministerial Regulation released in 2018, the current expense is 2% to 15% depending on the types of minerals. Most mining in Thailand has no more than 325 rai or 520,000 m² of mining permit boundary, as the

law requires that each plot not exceed the size of the above. Despite the large-scale mining, inspections are still under area-by-area inspections as outlined in the Mining Authorization Letter. Issued only by government agencies.

Mining is a misunderstanding of environmental destruction. Mining has led to changes in areas where mining is located. Yet, mining causes no disturbance to the environment and it doesn't destroy ecosystem. If the mine's owner follows the principles of the regulation, the principles of mineral waste will be included in the mining expense to take part in the social, economic and environmental impact prevention. Every category of mines and their sizes must be included in an Environmental Impact Assessment Report (EIA) before being allowed to operate. In addition, mines cannot be achieved without the acceptance of the society or the communities where the mining is nearby. Mining in the past has often caused environmental and aesthetic problems. This is domestically and internationally seen. This is partly due to a lack of conscience, lack of knowledge, lack of controlling laws, and mines in the past are very far away from the city. But we currently have a governing law, a responsible body, which requires concessionaires to take care of the prevention and the reduction of the environmental impact from mining industry and reclamation are normally having an important part of landscape architecture. Unlawful mining smuggling surveillance of officers may not be passed through by law enforcement.

2.2 Remote sensing

Remote sensing works through the reflection or radiation of objects on the earth's surface or nearby, providing identity or information of that object or area. The information is usually acquired form distanced visual data. We can establish the composition and nature of the earth's surface and atmosphere at local, regional, and global scales. Then, we can assess the changes by examining images taken at different points in time. In this aspect, remote sensing is important since it can provide geographical data that is difficult to obtained. Remote sensing is essential for visualizing (offering alternate and synoptic viewpoints) and characterizing human settings in the social sciences. Social science scholars routinely mix the sensed distance or its derivatives with other socioeconomic datasets within geographic

information systems to perform a spatial analysis [10]. Remote-sensing imaging equipment is classified into two types: Passive remote sensing and Active remote sensing [11].

2.2.1 Passive remote sensing

Solar radiation is used as a lighting source in passive remote sensing, such as hyperspectral and multispectral sensors. The visible, near-infrared, and shortwave infrared spectral areas are the main emphasis. Various satellites with multiple passive sensors onboard are flying above, and many more are being developed or planned to be launched in the following years. Some satellites of this system are Quickbird, WorldView-1, Landsat, THEOS, etc. Passive remote sensing satellites used in this study are Sentinel-2 and LandSAT-8.

2.2.1.1 Sentinel-2

Sentinel-2 has two working systems which are Sentinel-2A and Sentinel-2B. Sentinel-2A was initiated on June 23th, 2015, and Sentinel-2B was initiated on March 7th, 2017. Both satellites are a European multi-spectral imaging mission with a wide-swath and a high-resolution. The satellites are flying in the same orbit but the phased at 180° has a high review of 5-day frequency near the equator and every 2-3 days at the middle latitude according to all missions' requirements. The satellite has 13 spectral bands and three the spatial resolutions at 10 m, 20 m, and 60 m. At an altitude of 786 kilometers, the orbit is a sun-synchronous orbit with an average local solar time of 10:30 at the down node to the bosom, providing the sun's luminosity suitable for visual acquisition. Sentinel-2 products available to users are listed in Table 1 [12].

Table 1 SENTINEL-2 product types

Name	High-Level Description	Production and Distribution
Level-1C	Top-Of-Atmosphere reflectance in cartographic geometry	Systematic generation and online distribution
Level-2A	Bottom-Of-Atmosphere reflectance in cartographic geometry	Systematic and on-user side (using Sentinel-2 Toolbox)

Sentinel-2A level 1C was employed in this research that the level of 1C product has been made up to be 100 square kilometer tiles and ortho-images in UTM/WGS84 projection. The 1C level output has been created by projection the image in cartographic coordinates using a DEM. Of top of Atmosphere (TOA) reflectance, the image by pixel radiometric readings has been provided, together with all parameters needed to convert all of them to the radiance. Because of the original resolution of the different bands of spectral, Cloud Masks, land or water, and all of the ozone layer, the water vapor, and the pressure of mean sea level will be included in Level-1C products [13]. Sentinel-2 data is used in the Earth survey for Environment and Security program, which is run jointly by the European Commission and the European Space Agency and provides services such as forestry, agricultural production, land management, and, as same as humanitarian operations and disaster monitoring.

2.2.1.2 Landsat 8

Landsat 8 launched on February 11th, 2013, from Vandenberg Air Force Base, California, for an Atlas-V 401 rocket, with the extended payload fairing (EPF) from United Launch Alliance, LLC. (The Landsat 8 Launch in Quotes.) The Thermal Infrared Sensor (TIS) and the Operational Land Imager (OLI) are two science instruments on the Landsat 8 satellite payload (TIRS). These two sensors give seasonal coverage of the global landmass at 30-meter spatial resolution (visible, NIR, SWIR); 100-meter spatial resolution (thermal); and 15-meter spatial resolution (thermal) (panchromatic). NASA and the US Geological Survey collaborated in the development of Landsat 8. (USGS). During this time, the satellite was known as the Landsat Data Continuity Mission, and NASA was in charge of its design, production, launch, and on-orbit calibration (LDCM). The USGS took over routine operations on May 30th, 2013, and the spacecraft was renamed Landsat 8. At the Earth Resources Observation and Science (EROS) center, the USGS is in charge. Landsat satellite band designation shown in table 2.

Table 2 Landsat 8 band

Band name	Bandwidth (µm)	Resolution (m)
Band 1 (Coastal)	0.43 – 0.45	30
Band 2 (Blue)	0.45 – 0.51	30
Band 3 (Green)	0.53 – 0.59	30
Band 4 (Red)	0.64 – 0.67	30
Band 5 (NIR)	0.85 – 0.88	30
Band 6 (SWIR 1)	1.57 – 1.65	30
Band 7 (SWIR 2)	2.11 – 2.29	30
Band 8 (Pan)	0.50 – 0.68	15
Band 9 (Cirrus)	1.36 – 1.38	30
Band 10 (TIRS 1)	10.6 – 11.19	100
Band 11 (TIRS 2)	11.5 – 12.51	100

2.2.2 Active remote sensing

Active remote sensing employs a man-made radiation source as a probe, and the signal that have to returns to the sensor is utilized to characterize the atmosphere or the earth. The Synthetic Aperture Radar is a live system. It can emit radiation in a beam from a moving sensor in the microwave range and analyze the backscattered component that has returned to the sensor from earth surface. Satellites in this system such as ALOS, Sentinel-1, etc.

Sentinel-1 is the only active remote sensing source used in this study. The satellite is part of a two satellites constellation with the primary goal of the monitoring ground and sea. Following the retirement of ERS-2 and the termination of the Envisat program, the mission's purpose is to ensure C-Band SAR data continuity. The satellite will be equipped with a C-SAR sensor, which will provide medium and high-resolution imaging in all-weather circumstances. The C-SAR can capture night vision and detect minute movements on the earth surface, making it useful for land and maritime surveillance [14]. Acquisition mode in 4 special acquisition modes is Stripmap mode, Interferometric, Extra Wide Swath (EW), Wide Swat hand Wave. In

this study, IW mode was extraction DEM. 1 image per 1 sub-swath, per polarization channel, for a total of three or six photos, is included in the IW SLC product. Each sub-swath image is made up of a sequence of bursts, each of which was processed as its own SLC image. Individually focused complex burst images are combined into a single sub-swath image in azimuth-time order, with black-fill demarcation in between. Because the data has just one natural azimuth glance, adjacent bursts' imaged ground areas will only slightly overlap in azimuth - just enough to enable contiguous the cover of the surface. dislike SM and WV SLC products, which the sample of natural pixel that is spacing, all of the bursts in all sub-swaths of an IW SLC product are the resampled in the range and their azimuth to a common pixel for the spacing grids. The resampling to a common grid has been eliminated the need for further interpolation if the bursts have been merged to drive a contiguous earth surface range that detected images in final processing steps [15].

Sentinel-1's main acquisition mode over land is the IW swath mode. It has been collected data more than 250 km swath with a spatial resolution of 5 m by 20 m (single look). Terrain Observation with Progressive Scans SAR is used in IW mode to record three sub-swaths TOPSAR. In the TOPSAR approaching, the beam is automatically guided from back to front in the azimuth direction for each burst, eliminate result and scallop in homogenous images quality all the swath [17]. Each polarization channel in an IW SLC product has three sub-swath images, each of which is made up of a series of bursts shown in Figure 4.
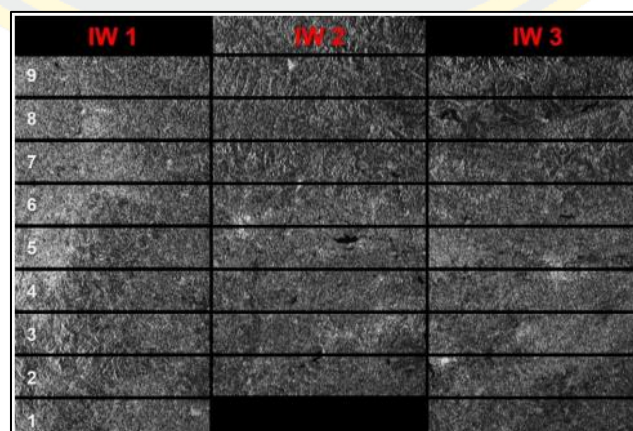

Figure 4 Sub-swaths (red text) and bursts (white text) [16]

Selection of suitable images for DEM generation has the following element:

- Short temporal baseline: To limit the danger of phase temporal decorrelation, the period between the two images should be a minimum number of days as possible. The signal is out of range and can no longer be exploited if surfaces change between the first and second acquisitions.

- Suitable perpendicular baseline, At the time of image acquisition, the distance between the satellites' locations should be between 150 and 300 meters. These topographic impacts on the differential phase are not as noticeable when the perpendicular is too tiny. With excessively large baselines, the coherent phase becomes increasingly divergent, resulting in decorrelation. However, the Sentinel-1 mission was designed primarily for deformation retrieval (DInSAR) rather than DEM creation. The majority of the baselines between two successive photos are less than 30 meters long. It can be difficult to discover image pairs with short temporal baselines and large perpendicular baselines.

- Suitable atmospheric conditions: Atmospheric water vapor causes phase delays and may degrade measurement quality. Therefore, it is recommended to choose photos taken during the dry season and to ensure that there is no rain between the two exposures.

2.3 Unmanned Aerial Vehicles

Unmanned Aerial Vehicle (UAV) is a remotely controlled aircraft or drone. It has many shapes and sizes. It uses automatic control which comes in two ways: automatic control from remote and automated control using manual flight systems that rely on existing computer programs. Complex systems are then installed in the aircraft. It can be said that unmanned aircrafts are aircrafts that can fly with automation without the need of pilots onboard. They may be equipped with high-quality cameras, both daytime cameras. Electro Optical and Infrared Sensor cameras that can record remote images and broadcast images. Signal to the monitor at the ground station. In the closest time to real time [17]. The image obtained from UAV were processed into an Orthophoto and DEM to be used in this study. Details of both data are as follows:

2.3.1 Orthophoto

Orthophoto is a landscape photograph where central projection is transformed into a perpendicular projection. In this way, with this change, it is possible to eliminate all planned distortions caused by the inclination of the aerial camera. There are also different distortions caused by the movement of respite, which eliminate the variation in the scale in the unresolved framework. These patterns are because of the differences inherent in the level of photographic terrain and the inclination that the camera may have at the time of the shooting. With this method of obtaining this information, it is possible to do one size and, of course, for the entire surface of the orthophoto to change the central projection to the right angle, which is useful to use a procedure called a correction. If this difference is significant, the correction will edit the three-dimensional model through the preliminary lines based on the unevenness of the terrain [18].

2.3.2 Digital Elevation Model

The Digital Elevation Model or DEM is used to explain the Earth's terrain and is a crucial factor in any procedure that uses digital topography analysis, including slope, curvature, roughness, and local relief, which are its derived properties. The criteria are typically used in a variety of applications, including flood risk simulation, landslide mapping, and soil volume calculation [19]. It is made up of a sampled array of heights for a variety of ground places at regular intervals. [20]. An example is shown in the Figure 5.
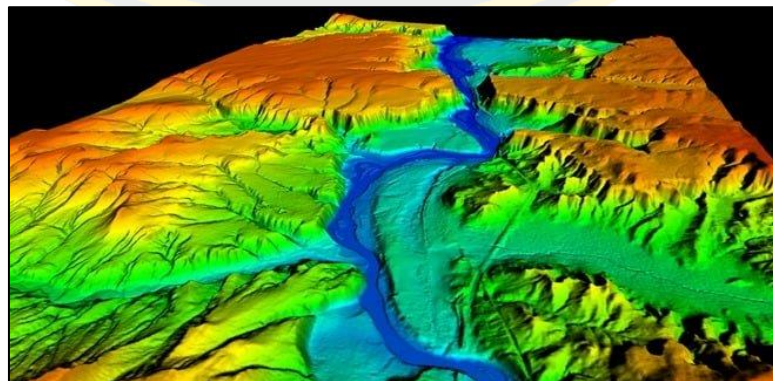

Figure 5 Digital Elevation Model

This study used The Terra Advanced Spaceborne Thermal Emission and Reflection Radiometer (ASTER) Global Digital Elevation Model (GDEM) Version 3 (ASTGM) as the reference DEM in the InSAR Back Geocoding and Enhanced Spectral Diversity procedure. The National Aeronautics and Space Administration (NASA) and Japan's Ministry of Economy, Trade, and Industry collaborated on the production of the ASTER GDEM data packages (METI). The Sensor Information Laboratory Corporation (SILC) in Tokyo creates the ASTER GDEM data packages [21]. The geographic coverage ranges from 83° North to 83° South and was created using ASTER images from March 1, 2000 to November 30, 2013. Version 3 was created with a spatial resolution of 30 m and is accessible in GeoTIFF format, same like the previous version. This data is freely available, and the study can be obtained at https://search.earthdata.nasa.gov/search [22].

2.4 Interferometric synthetic aperture radar: InSAR

InSAR (Interferometric Synthetic Aperture Radar) [23] is a technology that evolved from Synthetic Aperture Radar, or SAR, which was previously utilized in geological satellites. When radio signals strike the ground, they are reflected back to the satellite, where geological properties and topography reflect radio waves differently, allowing us to analyze the received radio waves and create a 3D map. InSAR is the application of SAR technology with Interferometry technology by combining information from two separate radar images with a predefined distance known as the perpendicular baseline. Based on the position of both satellites and their perpendicular baseline, 3-dimensional information of the Earth's surface can be recovered using the differing route lengths of the radar echo signal from a surface as received by both antennas to generate DEM or surface deformation maps. This approach is capable of assessing millimeter-level changes in deformation across time periods ranging from a day to a year. Its applications include geophysical monitoring of natural risks such as earthquakes. Landslides and surface deformation.

2.5 Research Review

Ugur Alganci, Baris Besol and Elif Sertel studied the DSMs generated from a range of satellite sensors were compared to examine their accuracy and performance [24]. They used three methods of accuracy assessment. In the first method, they selected 25 checkpoints from vacant land to assess the accuracy of DSM on the terrain surface. In the second method, about 1,000 checkpoints were randomly selected and used to assess the accuracy of the method for the entire study area. In addition, the control point method, vertical cross-sections are also drawn from the DSM to assess the accuracy associated with land cover, PHR and SPOT DSM have peaked.

Huifang Zhou and members [25] have studied, compared, and validated different DEM data derived from InSAR in Damxung area using two data derived from ERS-1 and ERS-2. They divided the processing into two types. In the first type they have not used the reference DEM in the InSAR DEM generation process, and the second method useed the reference DEM in the InSAR DEM generation process. They have found that the DEM derived from InSAR is feasible and effective, and then they confirmed that the accuracy of the InSAR generated DEM must be improved using external DEM. The second part testified that external DEMs play an important role in improving DEM accuracy.

Ioannis Kotaridis and Maria Lazaridou [3], Sentinel-2 imagery was used to delineate open-pit mining boundaries. The study area is the borders of a surface mining region located near Amyntaio town in northeastern Greece. Orfero toolbox (OTB) in QGIS software is the utility. The methodology begins with data processing and then moves on to picture segmentation. For the purposes of this investigation, the Mean-Shift segmentation algorithm was used. The segmentation was then evaluated using an unsupervised technique for various parameter values. It is paired with an autocorrelation index that indicates segment separability and variance, an indicator that depicts segment global homogeneity. The NDVI and its mean values were then calculated for each section. Finally, the mining area was retrieved by using spatial analysis methods such as the dissolve algorithm to aggregate segments that share a similar border.

Shunyao Wang and colleagues investigated the capability of detecting illicit mining activities by using the interferometric synthetic aperture radar (InSAR). The

method obtained the coherence coefficient from two SAR images obtained on different dates, then uses thresholding and filtering to create a decorrelation map, which is then overlaid with legal mining boundaries and optical satellite photos to detect illicit mining activity. The study area is in China's southwestern Inner Mongolia. This study demonstrates that InSAR coherence is suitable for detecting mining activities, and the method provide a novel strategy for detecting and monitor illicit open-pit mining [4].

Qianhan Wu and member investigated the application of TanDEM-X and SRTM DEMs, as well as spectral imaging for large-scale mining and automatic detection of opencast mining regions. Object-based image analysis and random forest (RF) methods were used. On the Landsat 8 sample data in Inner Mongolia, China, a sequence of threshold analysis, data preparation, picture segmentation, metric calculation, and influence factor regulation were created and analyzed. The total performance was excellent with the RF algorithm for the integrated DEM method of 7.54% and the only-optical pictures method of 12.70%. [6].

Andreas Braun [26] had studied the effects of limitations, most importantly, Temporal and perpendicular baselines of Sentinel-1 data selection in DEM processing. They were found that the acquisition of data from Sentinel -1 of the image pair had a minimum temporal baseline of 6 days, but it still had a significant impact on the rapidly changing area. Moreover, the acquisition of the two images has different dates, so it will also cause different weather conditions, which also affect the quality of the data. For the perpendicular baseline should be between 150 and 400 m to allow a precise description of topographic. But if there is a less temporal baseline, it will make the perpendicular baseline less too causes the resulting topographic data to have a high error value. In addition to these two factors, there are other factors: geometric and terrain factors at the landscape elevation, which also have a clear impact on the quality of InSAR measurements, such as areas near mountains with shadows. This shadow part causes an error value.

CHAPTER 3
MATERIALS AND METHODS

This chapter includes 3 sections, Data collection, Software and tools, and Methodology.

3.1 Data collection

The satellite data used in this study are freely available data, which are Sentinel-2, Landsat 8, and Sentinel-1. The validating data is from the governmental organizations which are responsible for reference data used in this study to ensure reliability and accuracy. DPIM's topographical mining data and DEM from RTSD are grouped into 2 parts for studying the horizontal changes (Table 3) and vertical changes (Table 4) in mining. The date and time that all satellite data were obtained with the data obtained by the UAV, which was used as a reference in comparison, had different time periods. But at this different time, the mining area where the study area has changed not much. Therefore, it does not affect the comparison of data.

Table 3 Detail of data for horizontal changing

Data	Round	Resolution	Date	Source
Orthophoto (UAV)	1	7.5 cm	Study area 1, 1 May 2018 Study area 2, 2 May 2018	Department of primary industries and mines
	2		Study area 1, 25 October 2018 Study area 2, 29 October 2018	
Sentinel-2 A	1	10 m	12 April 2018	https://scihub.copernicus.eu
	2		29 October 2018	
Landsat 8 Tier 1	1	MSS: 30 m	18 April 2018	https://earthexplorer.usgs.gov
	2	PAN: 15 m	27 October 2018	

Table 4 Detail of data for vertical changing

Data	Round	Resolution	Date	Source
DEM (UAV)	1	7.5 cm	Study area 1, 1 May 2018	Department of primary industries and mines.
			Study area 2, 2 May 2018	
	2		Study area 1, 25 October 2018	
			Study area 2, 29 October 2018	
RTSD DEM	1 and 2	30 m	19 April 1996	Royal Thai Survey Department
Sentinel-1 Level-1 SLC	1	5×20 m	3, 15 April 2018	https://search.asf.alaska.edu/
	2		12, 24 October 2018	

3.1.1 Base data

Orthophotos were used as a reference for validate the result of horizontal mining boundary changing. Meanwhile, DEM were used as a reference for validate the result of vertical mining boundary changing. Both orthophoto and DEM acquired by UAV. Because of it is highly accurate and accepted to be used in mining supervision in Thailand. RTSD DEM from RTSD is used for calibration DEM from InSAR technique. RTSD is the main agency responsible for producing the topographic map data of Thailand. The details of reference datasets used in this study are as follows:

3.1.1.1 Orthophoto (UAV)

Orthophoto data have ground sampling distance (GSD) of 7.5 cm. The geometric correction was done by Ground Control Points (GCPs) and surveyed by RTK GNSS.

For the study area 1 round 1, the RMSE in X-direction is 0.071 m and the RMSE in Y-direction is 0.135 m, shown in Figure 6. The red line in all the figures shown here is the boundary of mining according to the mining permit from DPIM.

The study area 1 round 2 have RMSE in X-direction of 0.015 m and in Y-direction of 0.012 m, shown in Figure 7.

The study area 2 round 1 have RMSE in X-direction of 0.024 m and in Y-direction of 0.053 m, shown in Figure 8.

The study area 2 round 2 have RMSE in X-direction of 0.019 m and in Y-direction of 0.021 m, shown in Figure 9.
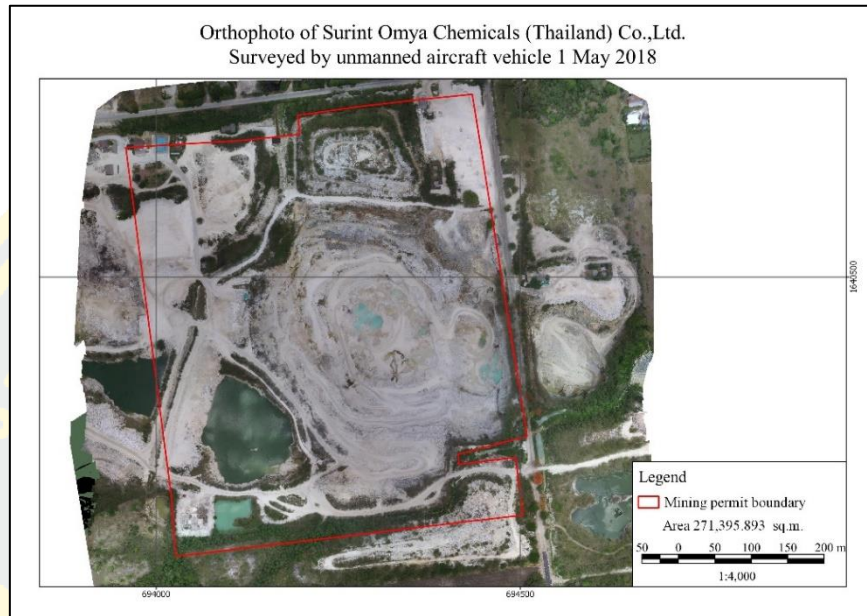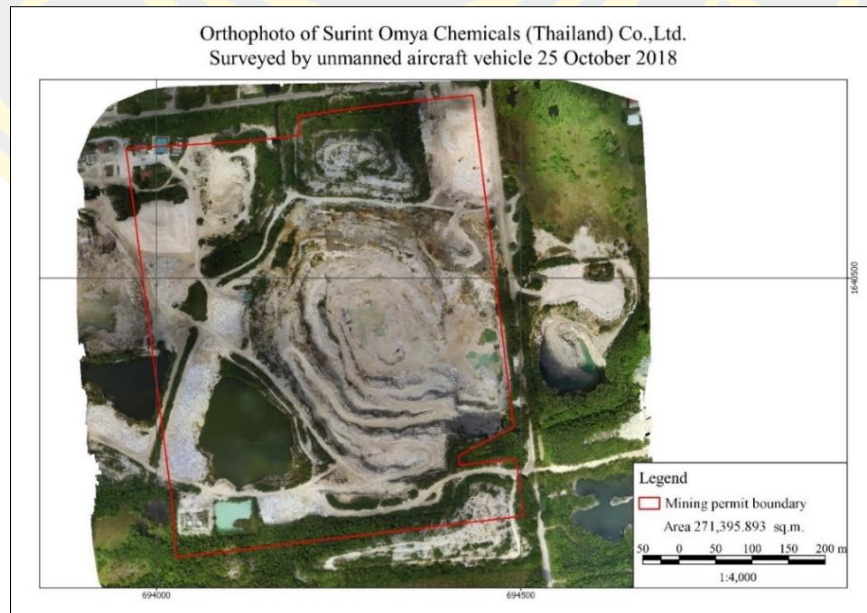

Figure 6 Orthophoto of study area 1 round

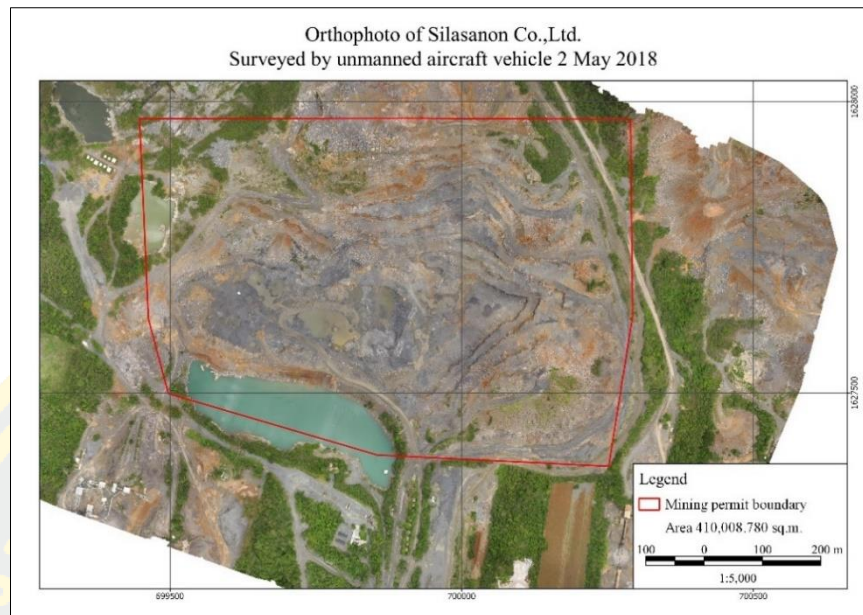**Figure 7** Orthophoto of study area 1 round 2

Figure 8 Orthophoto of study area 2 round 1

Figure 9 Orthophoto of study area 2 round 2

3.1.1.2 DEM (UAV)

DEM data have GSD of 7.5 cm and the geometry correction was done by GCP surveyed by RTK GNSS the same as the orthophotos. Study area 1 round 1 have

an RMSE of 0.157 m (Figure 10). Study area 1 round 2 have an RMSE of 0.060 m (Figure 11). Study area 2 round 1 have an RMSE of 0.038 m (Figure 12). Study area 2 round 2 have an RMSE of 0.048 (Figure 13).
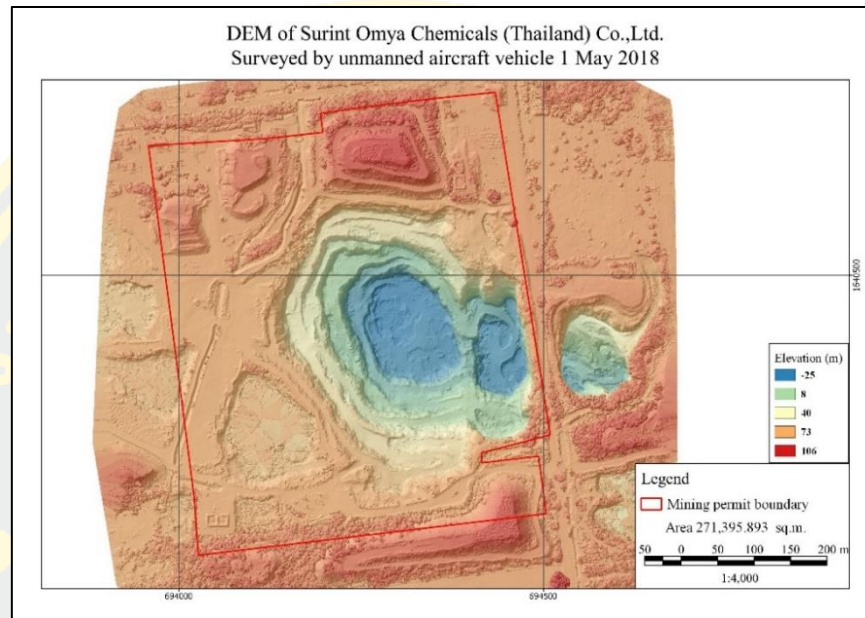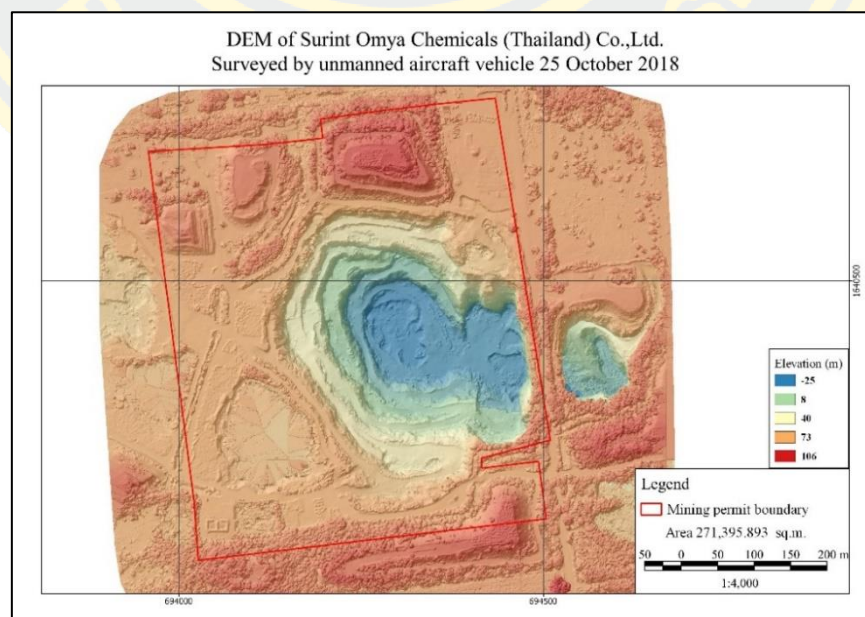

Figure 10 DEM of study area 1 round 1

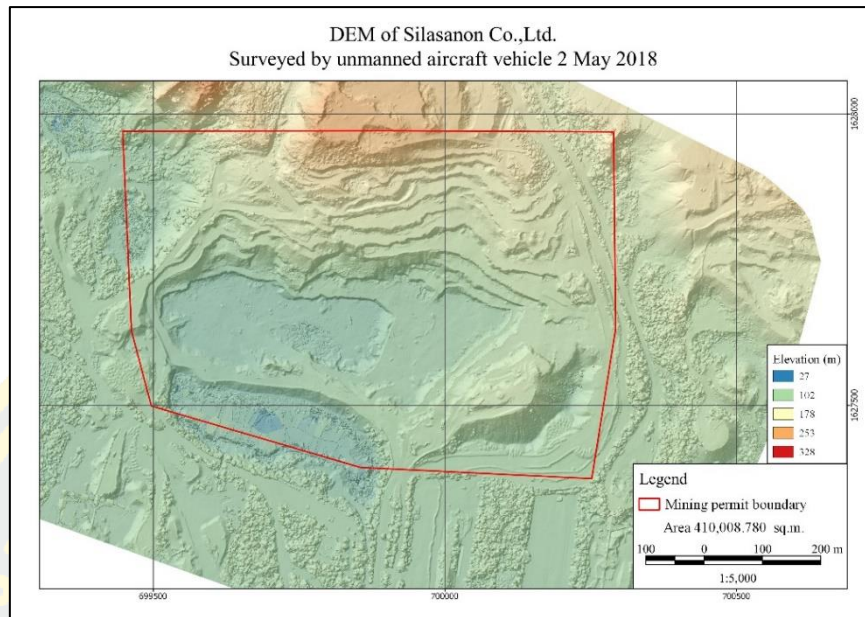**Figure 11** DEM of study area 1 round 2

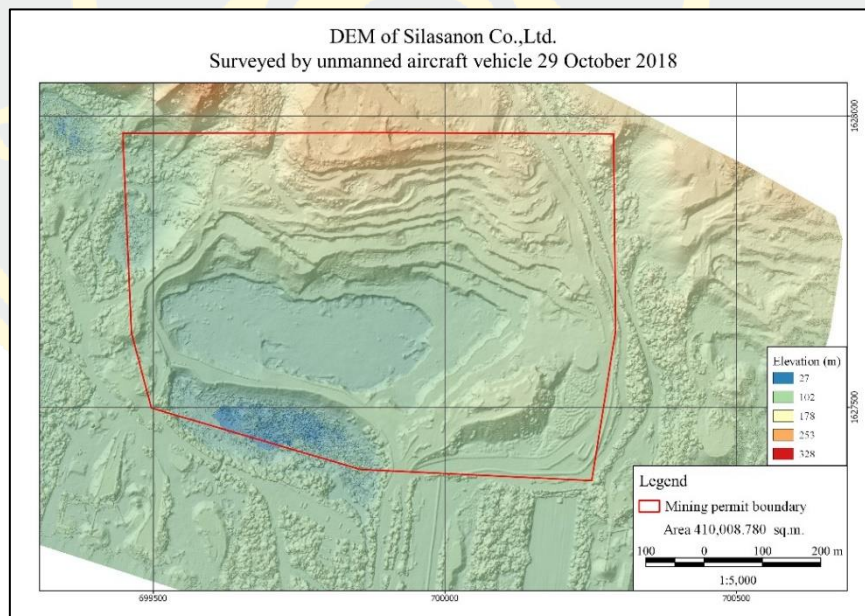**Figure 12** DEM of study area 2 round 1

Figure 13 DEM of study area 2 round 2

3.1.1.3 RTSD DEM

A digital elevation model data layer, which is under the supervision of the RTSD Royal Thai Armed Forces. Prepared as part of the project, the empowerment can be made to produce linear, code, or numerical maps. To map the scale of 1:50000 series L7018. In cooperation with the U.S. Mapping Agency, there is a horizontal coordinate referencing geographic coordinates on the WGS84 datum and the mean sea level (MSL) reference height value on the EGM96 geoid model are in meters. It covers the entire country of Thailand [27]. The DEM data used as a reference in this study is shown in Figure 14.
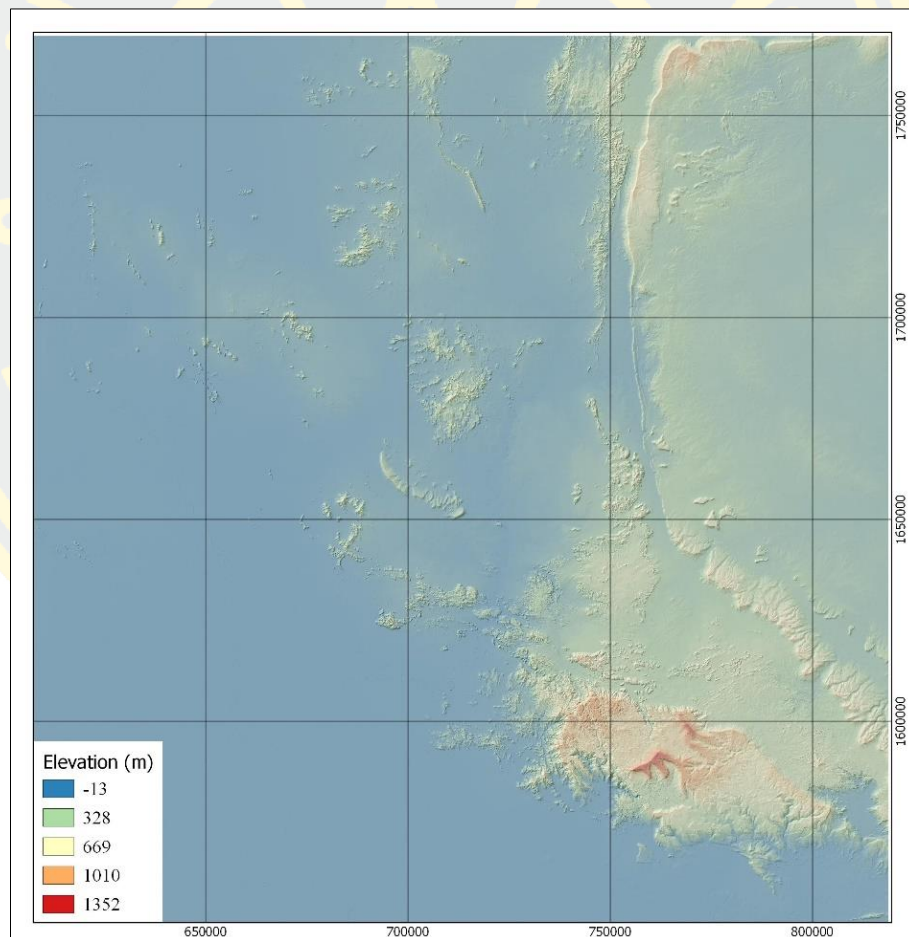

Figure 14 RTSD DEM

3.1.2 Sentinel-1

Sentinel-1 images were downloaded from the Copernicus Open Access Hub in Level-1 Single Look Complex (SLC) mode and Interferometric Wide (IW) acquisition mode at 250 km and 5×20 m resolution [28]. The polarization VV used for DEM generation in this study.

3.1.3 Sentinel-2

Sentinel-2 level 1C when adjusted Atmospheric Correction with Sen2Cor in SNAP software making level 2A data shown in Figure 15 and Figure 16.
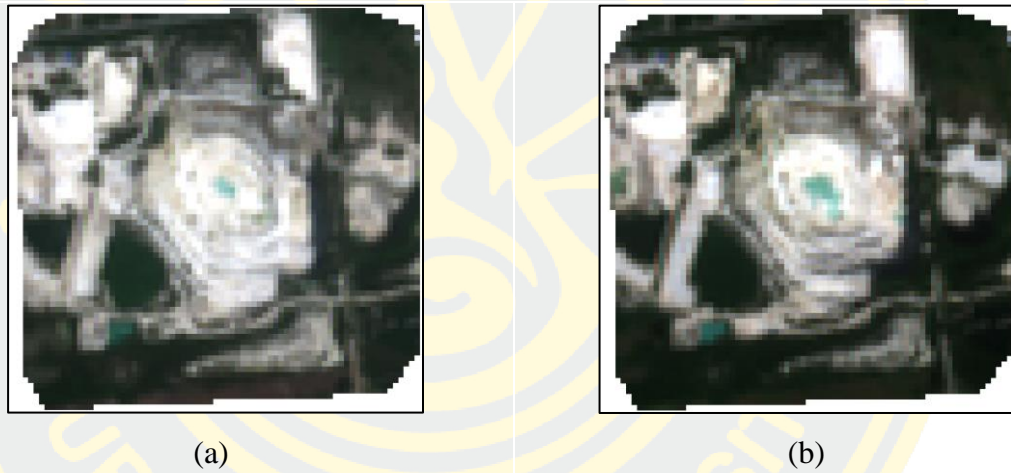

(a)   (b)

Figure 15 (a) Sentinel-2 image in study area 1 round 1, (b) study area 1 round 2
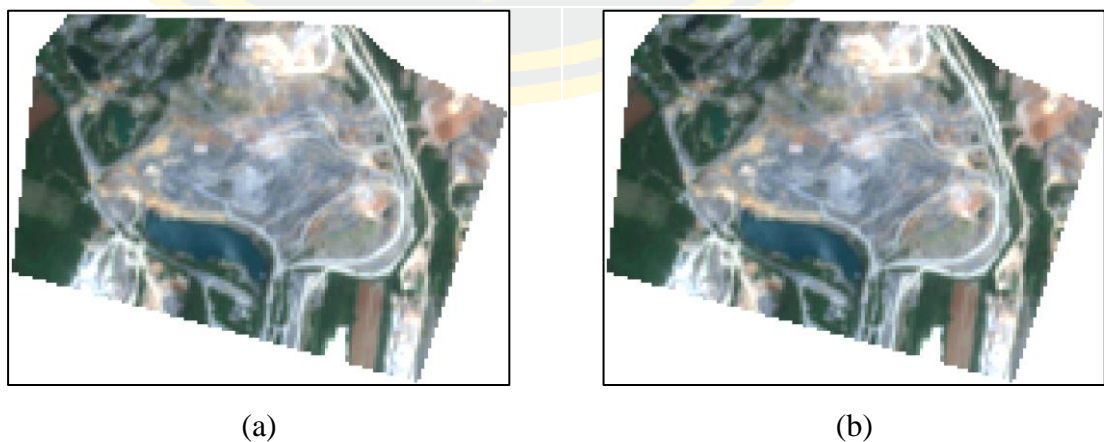

(a)   (b)

Figure 16 (a) Sentinel-2 imagery in study area 2 round 1, (b) study area 2 round 2

3.1.4 Landsat 8

This study used Landsat 8 imagery that has path 129, row 50, and could cover less than 20% shown in Figure 17 and 18.

(a)   (b)

Figure 17 (a) Landsat 8 imagery in study area 1 round 1, (b) study area 1 round 2

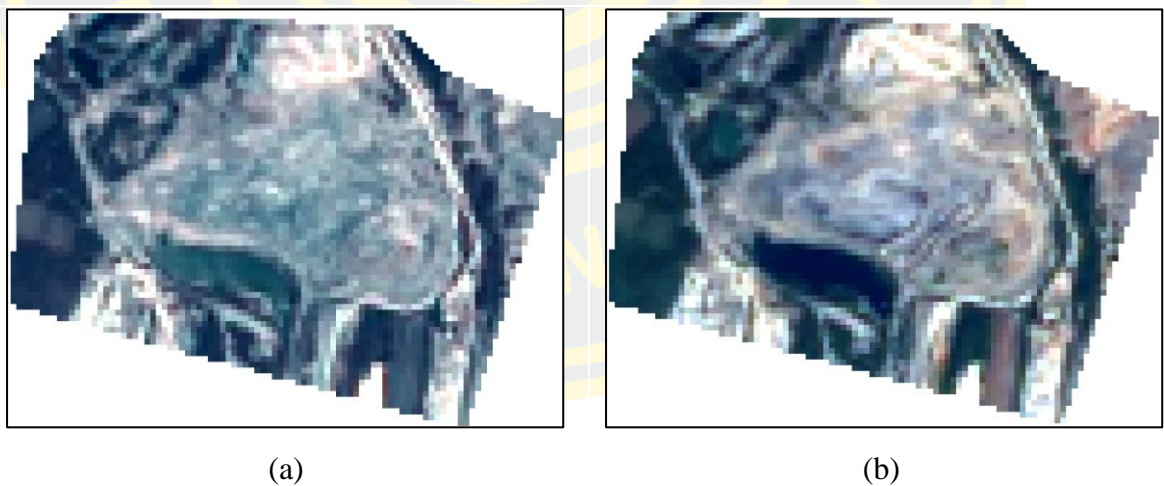(a)   (b)

Figure 18 (a) Landsat 8 image in study area 2 round 1, (b) study area 2 round 2

3.2 Software and tools

This study focuses on free-accessibility software consisting of SNAP (for processing data), Global Mapper (for analyzing vertical changes in mining), QGIS,

Orfeo Toolbox, and SCP plugin QGIS (for process data from optical remote sensing and extracting the mining boundary, the horizontal changes in mining).

3.2.1 SNAP Software

The Sentinel Application Platform (SNAP) is a unified architecture that underpins all Sentinel Toolboxes. Brockmann Consult, Skywatch, Sensar, and C-S created the software. Because of the following technological breakthroughs, the SNAP architecture is appropriate for Earth observation (EO) processing and analysis: extensibility, portability, a modular rich client platform, generic EO data abstraction, tiled memory management, and a graph processing framework. Other than Sentinel sensors, SNAP and the separate Sentinel Toolboxes support a wide range of sensors. ESA/ESRIN is making the SNAP user tool available to the Earth Observation Community for free [29].

3.2.2 Global Mapper Software

Global Mapper is a powerful and reasonably priced geographic information system (GIS) tool that integrates a wide range of software solutions for spatial data processing and provides access to a variety of formats used in the worlds of CAD, GIS, and engineering. Through rapid data processing, accurate mapping, and optimal spatial data management, businesses and organizations of all sizes will quickly experience a considerable return on investment [30].

3.2.3 Quantum GIS Software

QGIS is a Geographic Information System that is free and open source. The project has begun in 2002 May and launched as a Source Forge project in June of that year. They have worked tirelessly to make GIS software accessible to everybody with a computer. The software is intended to be an easy-to-use GIS, with common functions and capabilities. The project's initial goal was to create a GIS data viewer. QGIS has progressed to the point that it is used for daily data capture, GIS data viewing, complex GIS analysis, and presentations in the form of sophisticated maps, atlases, and reports. QGIS supports a wide range of raster and vector data formats, and additional format support can be quickly added by utilizing the plugin architecture [31].

3.2.4 Orfeo Toolbox

Orfeo ToolBox (OTB) [32] is an open-source remote sensing project for state-of-the-art. It was built onto the shoulders of the open-source geospatial community and can process terabyte-scale optical, multispectral, and radar pictures. There are numerous applications accessible, ranging from ortho-rectification or pan-sharpening to categorization, SAR processing, and much more. QGIS, a free and open-source GIS that facilitates the generation, modification, visualization, and dissemination of geospatial data, was used for spatial analysis methods [33].

3.2.5 Semi-Automatic Classification Plugin

The Semi-Automatic Classification Plugin (SCP) is a free open-source plugin for QGIS that allow semi-automatic also known as supervised classification of remote sensing imagery. It includes numerous tools for downloading free images such as Sentinel-2 and Landsat 8 that used in this study, preprocessing, postprocessing, and raster calculation [34].

3.3 Methodology

The methods used in this study are shown in Figure 19. They are divided into 3 parts consisting of data preprocessing, comparison and validation, and the results were used to assess the suitability for application in small-scale mining operations.
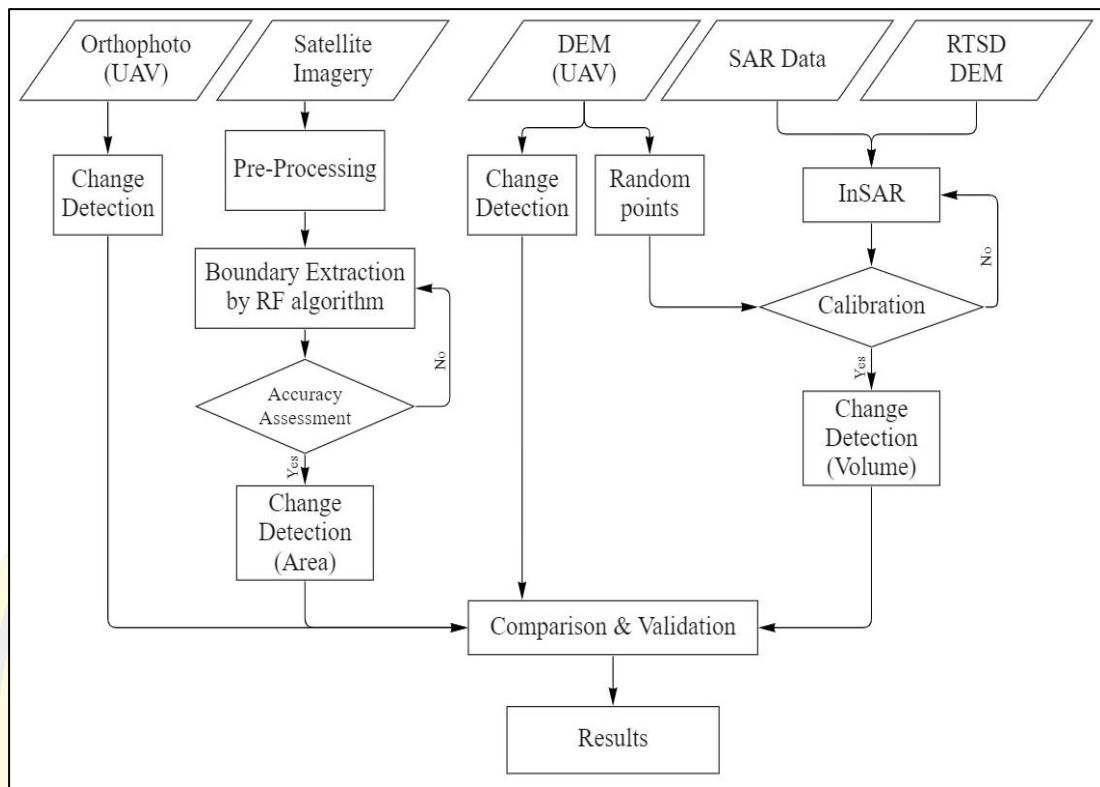
Figure 19 Flowchart of method

3.3.1 Pre-Processing

The SCP plugins in QGIS software were used for preprocessing of optical satellite images in this study as follows:

Sentinel-2 Level 1C data were downloaded from URL: https://scihub.coper nicus.eu using SCP plugins and I corrected the accompanying error. The first step is atmospheric correction. And next, resample all bands to 10 m. Because Sentinel-2 has three different geometric resolutions which are 10 m, 20 m, and 60 m, I combined the bands and clip the image only in the study area. Finally, is to have a geometric correction to correct the distortions and make all the data in the same coordinates and projection as well.

Landsat 8 preprocessing starts with atmospheric correction, then combining the bands and pan-sharpening images to convert them from 30 m resolution to 15 m and clip the image only in the study area. Finally, for the geometric correction in study area 1 and study area 2, five GCP data per area based on orthophoto data

produced from UAV data were used to modify satellite data at the same location and coordinates and were used as references. If this is not done at this stage, the comparison and the results of the study will be erroneous.

For the SAR data, Sentinel-1 IW Level 1 Single Look Complex (SLC) product was downloaded data from Copernicus Open Access Hub web interface. The products used in this study were in the IW mode which has a resolution of 5x20 meters, descending orbit, and 12 days period between pair image.

3.3.2 Boundary Extraction

To extract the mining boundaries, segmentation by mean-shift algorithm is used. Then, RF algorithm is used to classify the data into 5 classes; mining area, bare soil, road, water, and vegetation. Then visually modify the boundary of the mining for that the data is more accurate based on the real boundary from UAV data and dissolve the classes into two classes: mining and non-mining areas. Lastly, a validation of the classification was performed. As shown in Figure 20.
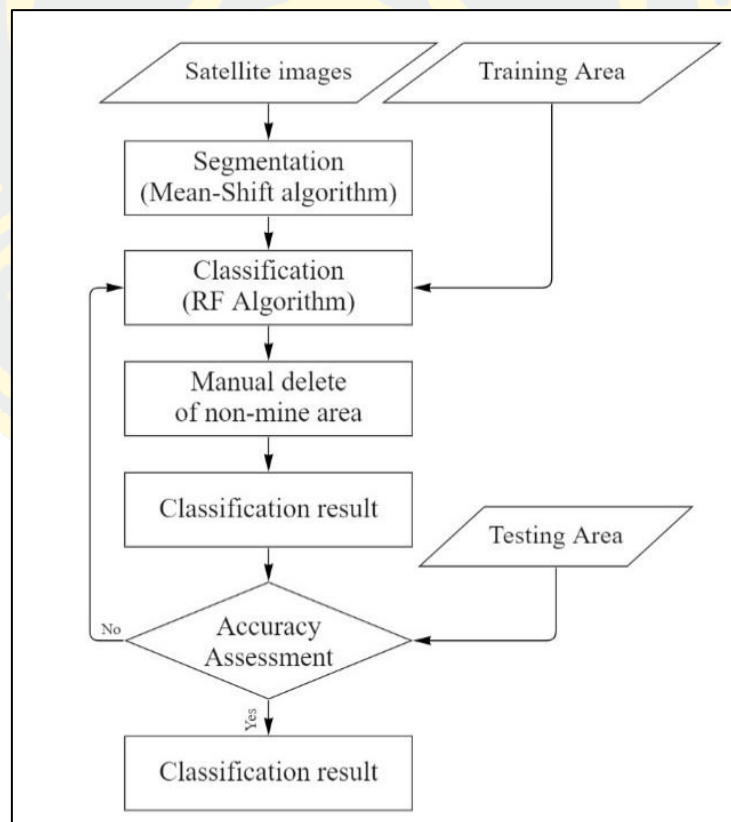

Figure 20 Flowchart of boundary extraction

3.3.2.1 Image Segmentation

The Mean-Shift segmentation algorithm was used. It is a popular non-parametric clustering method in image analysis. [35]. Mean-Shift segmentation algorithms have shown sufficient results regarding to digital number grouping [36]. It is capable of handling various remote exploration satellite data for sample images with medium or high spatial resolution. The simplicity of the filtering procedure is a key element in its appeal. The multidimensional nature of the problem and the existence of numerous implementations [37]. This study used the OTB in QGIS software for segmentation operator.

3.3.2.2 Random Forest Algorithm

A variety of supervised classification techniques can be used to assign pixels in an image to different map classes. Random forest (RF) was used in this study. The features used to train any statistical model should be thoroughly thought out and informed by your knowledge of the phenomenon of interest [35]. Random forest is a machine learning algorithm that is particularly popular in remote sensing. For each pixel, a Random Forest algorithm generates a large number of decision trees. Each of these decision trees casts a vote on how to classify the pixel. The map class for that pixel is subsequently assigned to the land cover class with the greatest votes. When compared to other classification techniques, random forests are more efficient and accurate on large datasets [38]. RF algorithms are defined in vector classifier operators using OTB, as well as the segmentation processing.

3.3.2.3 Validation and Accuracy Assessment

The performance of the classification result was assessed based on the formed confusion matrix using the 32 observations for study area 1 and 34 observations for study area 2 from the test samples. The overall accuracy was calculated using the confusion matrix. I created a confusion matrix for global accuracy and analysis of the reliability of the implemented models. I calculated the kappa statistic for algorithm evaluation, which tests the success of pairs of data between a set of categories while correcting the success expected probability. The values ranging from -1 and +1. The value of -1 shows a complete disagreement between the categories and the value of +1 shows a perfect agreement [39].

3.3.3 InSAR technique

DEM extraction from Sentinel-1 data using InSAR techniques according to the manual of DEM generation with Sentinel-1 challenges and workflow from SkyWatch Space Applications Inc. [16] consists of 10 main steps: 1) TOPSAR-Split, 2) Apply-Orbit, 3) Back-Geocoding, 4) Enhanced-Spectral-Diversity, 5) Interferogram, TOPSAR-Deburst, Topographic Phase Removal, Goldstein Phase Filtering, Snaphu Unwrapping, Phase to Elevation, and Range Dropper Terrain Correction. An overview of the steps is shown in Figure 21.

3.3.3.1 TOPS Split

As the first step in extracting DEM, S-1 TOPS Split has been applied to the selected data only those bursts which are required for the analysis. For this process, the SLC Level-1 product of IW with VV polarization was chosen. The image is divided into vertical columns or swaths and then horizontal rows or bursts to contain only the area of interest required for analysis which greatly reduces the computer time for each additional step.
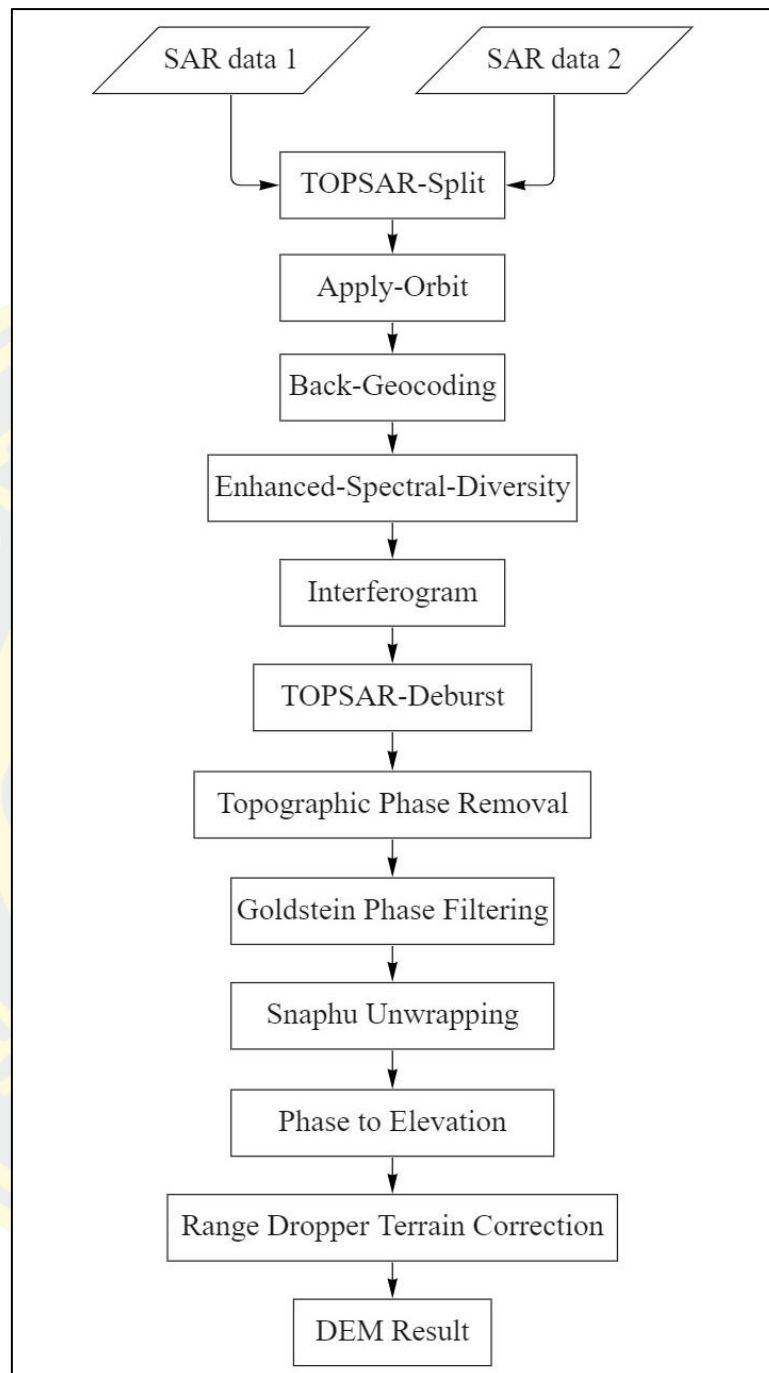
Figure 21 Flowchart of calibration method

3.3.3.2 Applying Orbit Information

The next step is to apply the orbit file to each image which contains the precise information of the 3-D orientation of the satellite in orbit as well as pitch, roll,

and yaw. Orbit auxiliary data contain information of the satellite's position during SAR data collecting and are added to its metadata using the Apply Orbit File operator.

3.3.3.3 Back Geocoding and Enhanced Spectral Diversity

The S-1 Back Geocoding operation co-registers the two split products using the orbit information provided in the previous phase and data from a digital elevation model (DEM) retrieved by SNAP. This stage is critical because the correction of the topographic effects of the SAR images backscatter is required [40]. The images are referenced to a DEM. DEM referenced in the processing is ASTER GDEM version 3 with a spatial resolution of 30 m.

3.3.3.4 Interferogram Formation and Coherence Estimation

The interferogram has been created by multiplying the master image by the complex conjugate of the slave. The amplitude of the images is multiplied, meanwhile the phase shows the phase difference between the two images.

3.3.3.5 TOPS Deburst

The interferogram product remove the seamlines between the single bursts. The output includes the same bands as the input, but with merged bursts based on their zero Doppler time. This also contributes to faster the processing time and obtain higher data accuracy.

3.3.3.6 Goldstein Phase Filtering

Noise from temporal and geometric volume scattering, decorrelation, and other processing errors can all degrade interferometric phase. Although phase information in decorrelating areas cannot be restored, the quality of the interferogram's fringes can be improved by using specific phase filters. For example, the Goldstein filter utilizes a Fast Fourier Transformation (FFT) to improve the image's signal-to-noise ratio. This is necessary for successful unwrapping in the following step.

3.3.3.7 Phase Unwrapping

The interferometric phase in the interferogram is ambiguous and known as the scale of 2π. The interferometric phase must first be unwrapped in order to be related to the topographic height. The altitude of ambiguity was defined as the altitude difference that results in an interferometric phase change of 2π after flattening the interferogram.

3.3.3.8 Phase to Elevation

The unwrapped phase is a continuous raster that is still not a metric measure. To convert the radian units into absolute heights. It translates the phase into surface heights along the line-of-sight (LOS) in meters. The LOS is the line between the sensor and a pixel. A DEM is used to put the elevation values in the correct level.

3.3.3.9 Terrain Correction

Terrain Correction is done by correcting SAR geometric distortions with a digital elevation model (DEM) and generating a map-projected product.

3.3.3.10 Reprojection

Reprojection modifies the coordinate system of data obtained from the InSAR process to the same coordinate system as the referenced data. It uses the Universal Transverse Mercator (UTM) World Geodetic System (WGS) 1984 zone 47 north coordinate system, which is a coordinate system used in Thailand.

3.3.4 Calibration and Accuracy assessment

The statistics approach used in this process consist of calculating the RMSE and the R^2. For calibration, the height difference between the RTSD DEM and DEM were obtained from InSAR technique after projecting them to the same coordinate system and sampling them to the same spatial resolution. This was done by using random points of 506 checkpoints determined from an unchanged area of the terrain and extracting the values from the RTSD DEM for the elevation checking. When the accuracy is verified, if it is found that there is still a high error, the DEM is corrected using the average value of the error, and the difference between the two layers of data is corrected with the raster calculator by correcting it with the same values of the entire area. For example, when verifying the accuracy of the data, the DEM obtained from the InSAR technique has a mean error of 20 m from the RTSD DEM, which indicates that the DEM obtained from the InSAR technique has an elevation value that is 20 m lower than the reference DEM. Therefore, the revision will take 20 m plus added to the DEM obtained from the InSAR technique, to provide an additional 20 m elevation of DEM data obtained from InSAR techniques making data closer to reference. The last step is the process of evaluating accuracy using 100 random points from the UAV DEM in two areas and two rounds. The calibration and accuracy assessment step are shown in Figure 22.
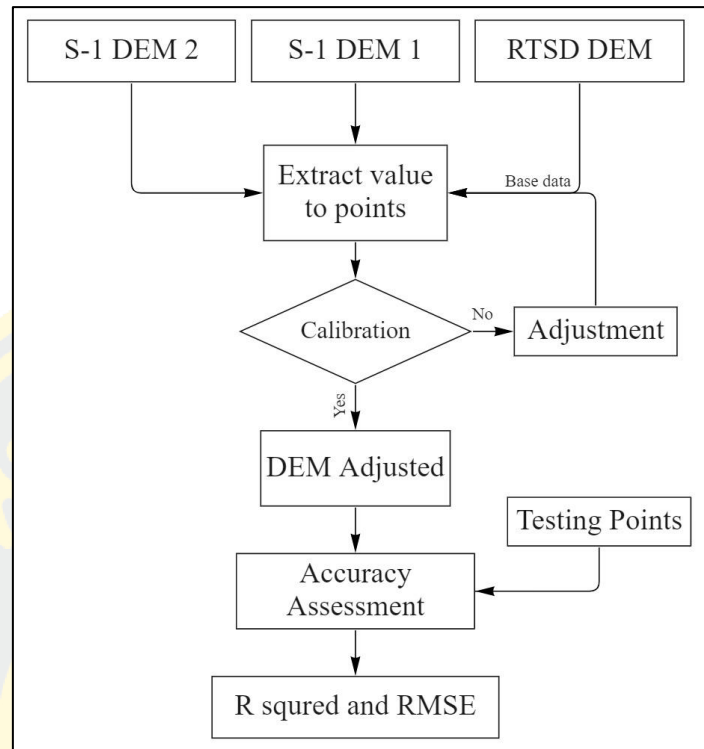
Figure 22 Flowchart of calibration method

3.3.4.1 Root Mean Square Error (RMSE)

The standard deviation of the residuals is represented by the RMSE (prediction errors). Residuals are a measure of how far away the data points are from the regression line; RMSE is a measure of how spread out these residuals are. In other words, it indicates how concentrated the data is around the line of greatest fit [41]. The RMSE value was calculated from this formula:

$$RMSE = \sqrt{\frac{\sum_{i=1}^{n}(y_1 - \hat{y}_i)^2}{n}} \tag{1}$$

3.3.4.2 R-Squared

R-Squared, often known as the coefficient of determination. It can have values in the range of $(-\infty, 1]$ based on the relationship between the ground truth and the prediction model [42]. A value of 1 indicates that the predictions are identical to the observed values; a value of R2 greater than 1 is not possible. A value of 0 indicates that there is no linear relationship between the observed and predicted values, where "linear" in this context means that a non-linear relationship between the

observed and predicted values is still possible. Finally, A value of 0.5 indicates that the model explains half of the variance in the outcome variable [43]. The correlation coefficient is given by the formula:

$$R^2 = \left(\frac{n(\Sigma xy) - (\Sigma x)(\Sigma y)}{\sqrt{[n\Sigma x^2 - (\Sigma x)^2][n\Sigma y^2 - (\Sigma y)^2]}}\right)^2 \qquad (2)$$

3.3.5 Change Detection and Comparison

3.3.5.1 Horizontal

The analysis of change detection of horizontal mining compared the boundaries of horizontal mining obtained by UAV and the boundary extraction process. The data was analyzed for changes in 2 periods using Land cover change operator in SCP plugin in QGIS software. The input data in this step has 12 layers and when the changes area is analyzed, the data is exported into 6 layers. The horizontal change detection steps are shown the flowchart in Figure 23.
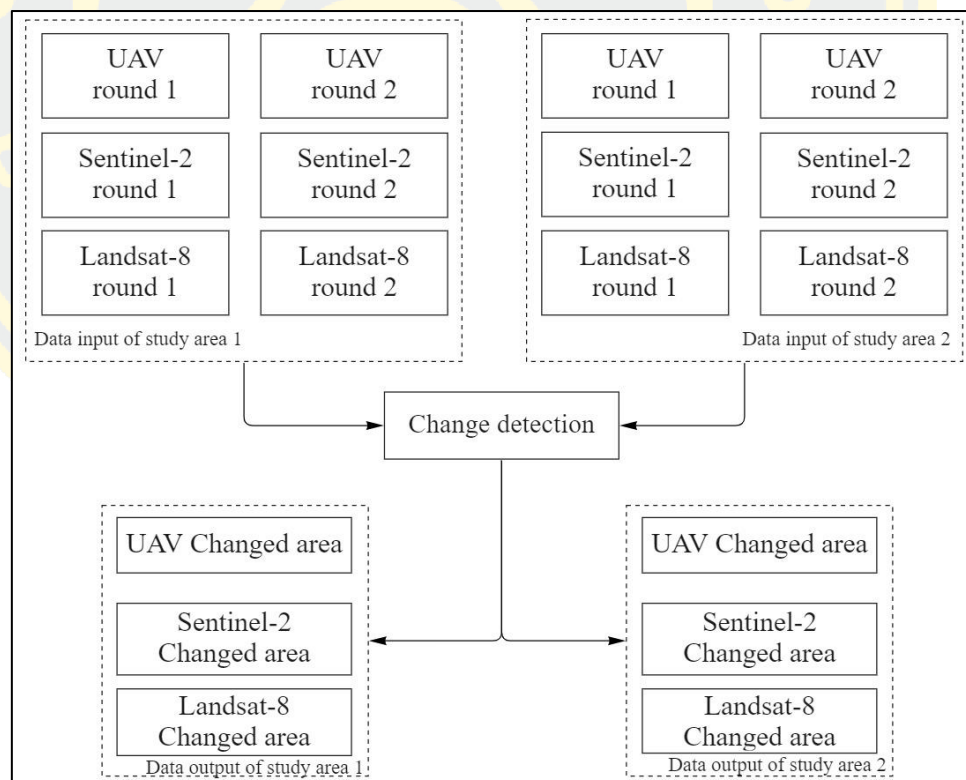
Figure 23 Flowchart of horizontal change detection

3.3.5.2 Vertical

Analyzing changes in vertical mining using DEM data obtained from InSAR technique and analyzing the volume changes of two periods using measure volume between the surface operator in Global Mapper software. Before analyzing the volume change, the resolution of the UAV DEM is adjusted to a resolution of 14 m so that all datasets have the same resolution since the DEM data from the UAV has a resolution of 7.5 cm, but the DEM from the InSAR technique has a resolution of 14 m. The step of this process is shown in Figure 24.
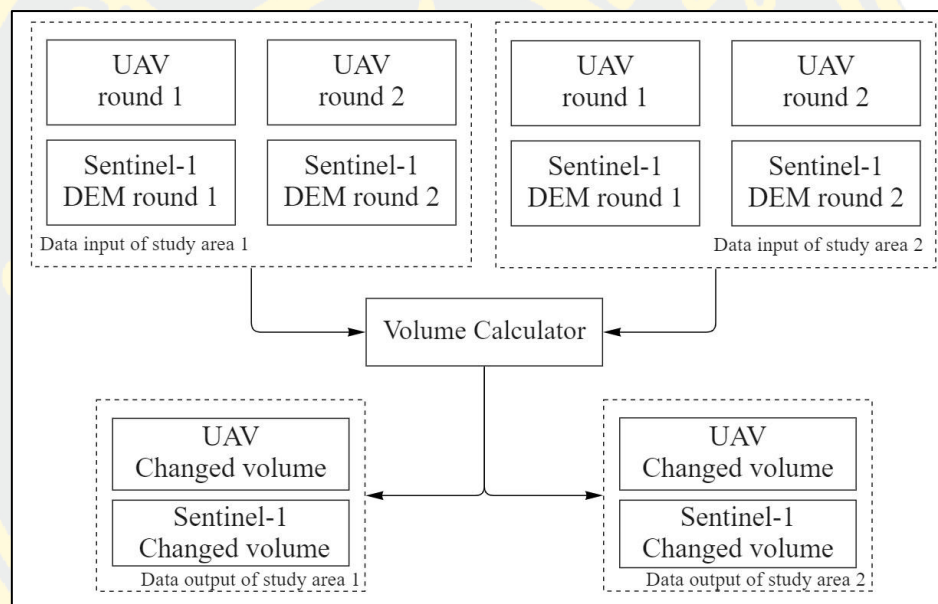
Figure 24 Flowchart of vertical change detection

CHAPTER 4
RESULTS AND VALIDATION

The study of change detection for surface mining boundary both horizontal and vertical directions based on multi-source remote sensing images is conducted in 2 mining areas consists of study area 1, Calcite mining in Lopburi Province, with an area of 271,395.893 m², and study area 2, Industrial stone in Saraburi Province, has an area of 410,008.780 m² This study is mainly focused on the application of readily available tools such as open-sources software and freely available satellite data for extracting horizontal boundary of surface mining from Sentinel-2 and Landsat-8 satellite imagery by segmentation by Mean-Shift segmentation algorithm and supervised classification using RF Algorithm with a plugin in QGIS software, and DEM extraction from SAR using InSAR technique. Processing by SNAP software and. Follow by change detection of mining then compare the difference with data collected from UAV. Finally, the result is then assessed for establishing and improving the guideline of the application of satellite technology for change detection of surface mining, which consists of three aspects as follows:

4.1 Boundary Extraction
4.2 DEM Extraction and Calibration
4.3 Change Detection

4.1 Boundary Extraction

The result of mining boundary extraction from segmentation with Mean-Shift Segmentation algorithm and classified with RF algorithm are classified into two types: mining area and non-mining area, with the brown area, representing the mining area and gray area representing the non-mining area. For accuracy assessment using the 32 observations for study area 1 and 34 observations for study area 2 from the test samples, based on a reference from the UAV. The kappa statistic is used to calculate overall accuracy. This result can be categorized by the source of satellite data as follow:

4.1.1 Boundary extraction from Sentinel-2 imagery

The result of mining boundary extraction from Sentinel-2, first mining in study area 1, covered area of 72,600.000 m² Second mining in study area 1 covered area of 80,700.000 m². While first mining in study area 2 covered area of 237,400.000 m² and second mining in study area 2 covered area of 253,708.789 m² with the overall accuracy of 95.66%, 97.47%, 100%, and 99.26% respectively. The results are shown as Figure 25 to 28.
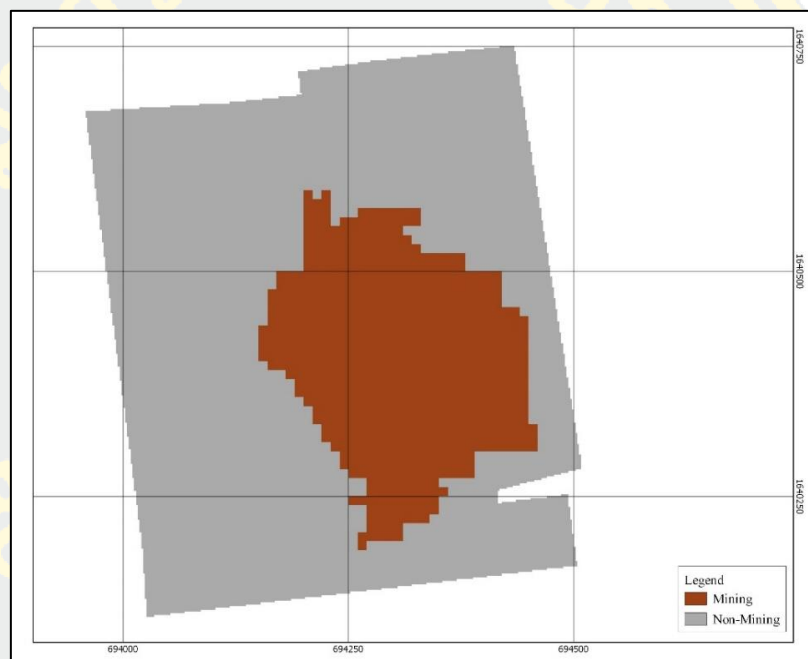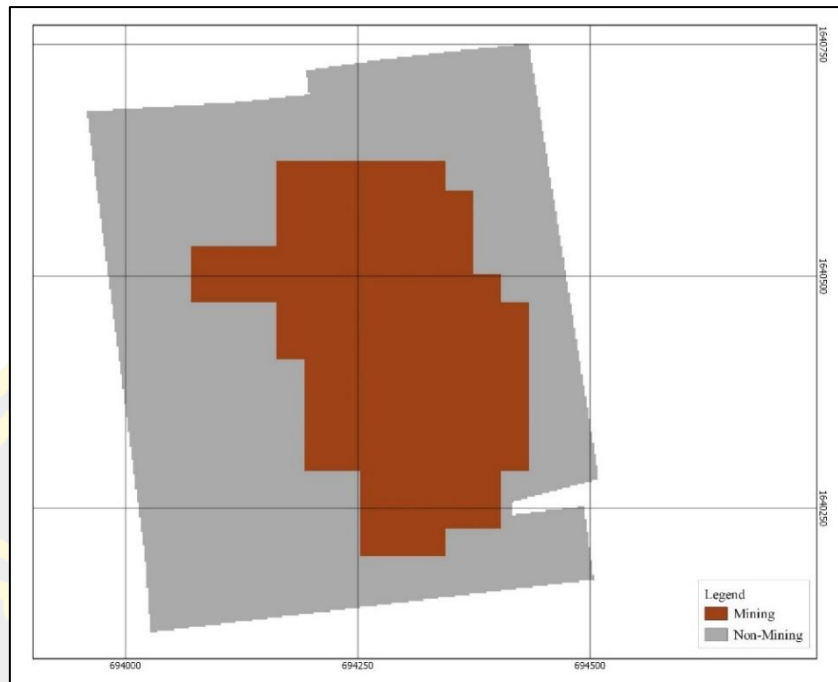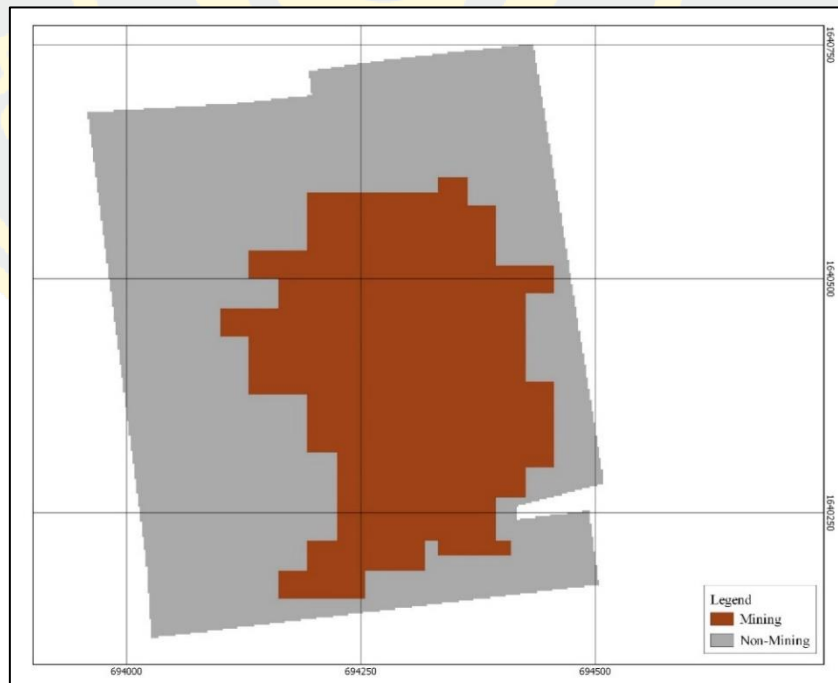

Figure 25 Boundary of study area 1 round 1
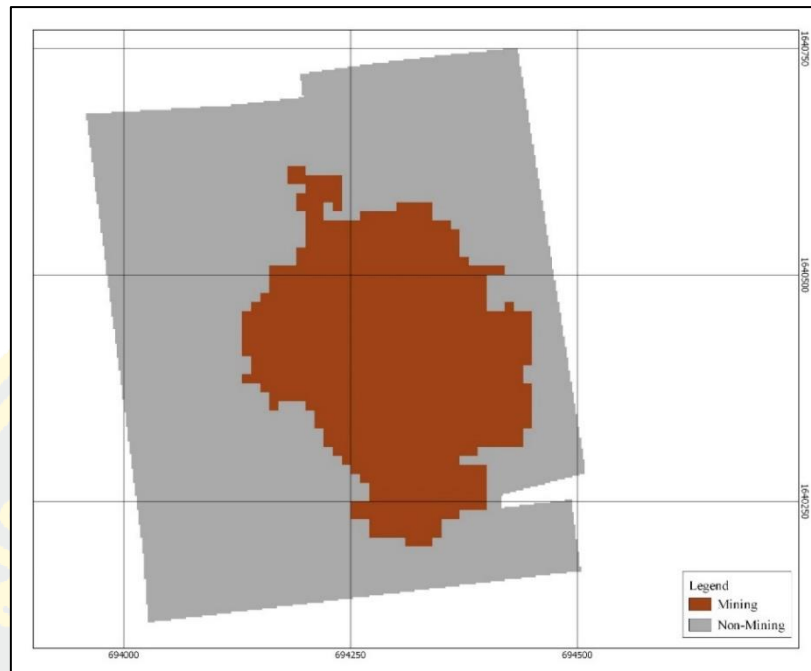
Figure 26 Boundary of Study area 1 round 2
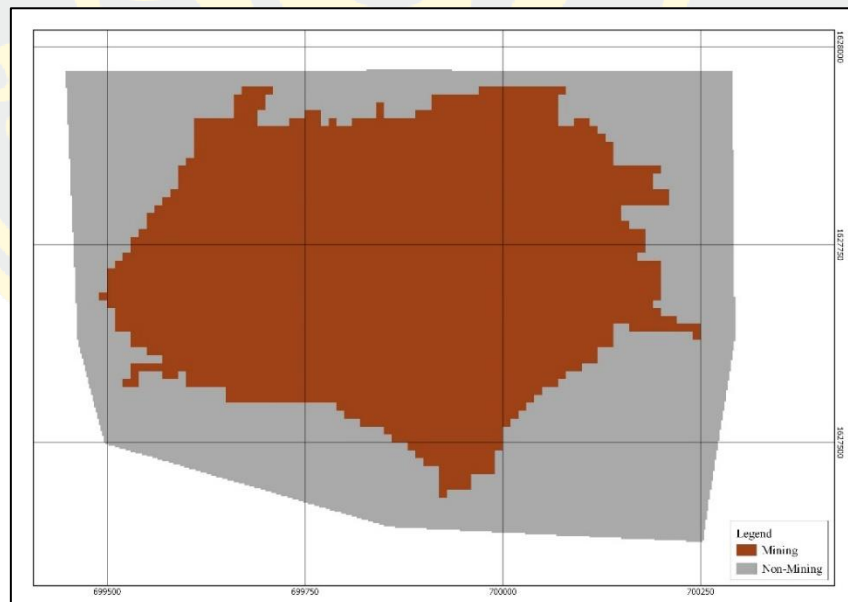
Figure 27 Boundary of study area 2 round 1
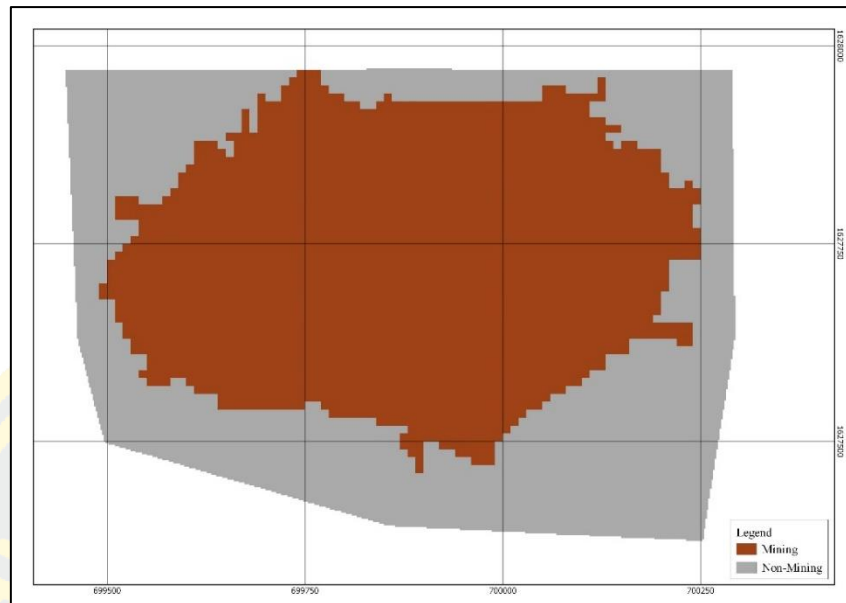
Figure 28 Boundary of study area 2 round 2

4.1.2 Boundary extraction from Landsat 8 imagery

The result of mining boundary extraction from Landsat 8 satellite reveals that in first mining in study area1 covered area of 95,908.760 m², second mining in study area1 covered area of 101,570.418 m² Meanwhile, first mining in study area2 cover area 234,583.948 m² and in second mining in study area 2 covered area of 240,300.000 m² Overall Accuracy are 86.57%, 96.50%, 99.35%, and 95.90% respectively. The results are shown as Figure 29 to 32.

Figure 29 Boundary of study area 1 round 1
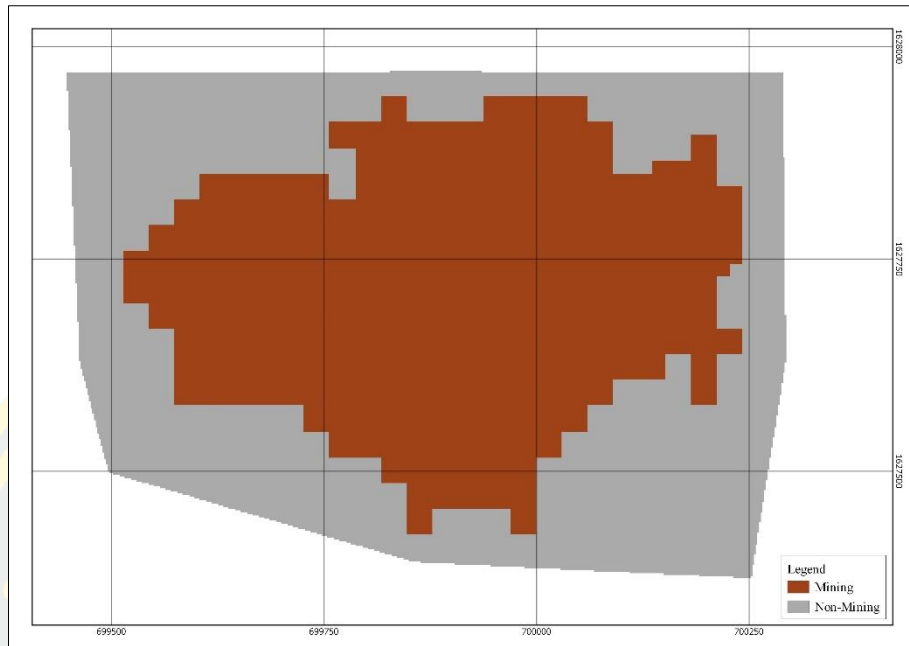

Figure 30 Boundary of study area 1 round 2

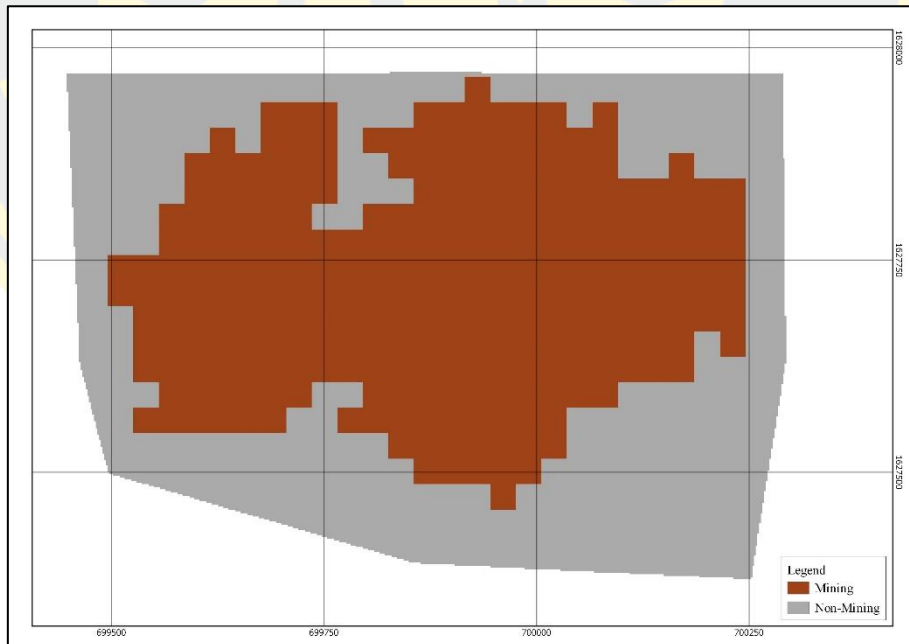**Figure 31** Boundary of study area 2 round 1

Figure 32 Boundary of study area 2 round 2

4.2 DEM Extraction and Calibration

This procedure consists of the results of DEM obtained through InSAR technique processing, then calibration with RTSD DEM and adjust DEM obtained InSAR technique. After adjusting, The DEM will be clip by the boundary of the study area for the validation. Finally, analysis of volume changes in the next step.

4.2.1 DEM Extraction

The process of DEM extraction using two pairs of satellite image from Sentinel 1 SLC product which are the data from 3 April and 15 April 2018. The duration is 12 days in time range with 70.25 m of perpendicular baseline. And another pair of satellite imagery is the data from 12 October and 24 October 2018. The duration is 12 days in time range with 60.43 m of perpendicular baseline. Using InSAR technic with SNAP software processing. DEM obtained after all of the InSAR process is shown as shown in Figure 33 and 34.
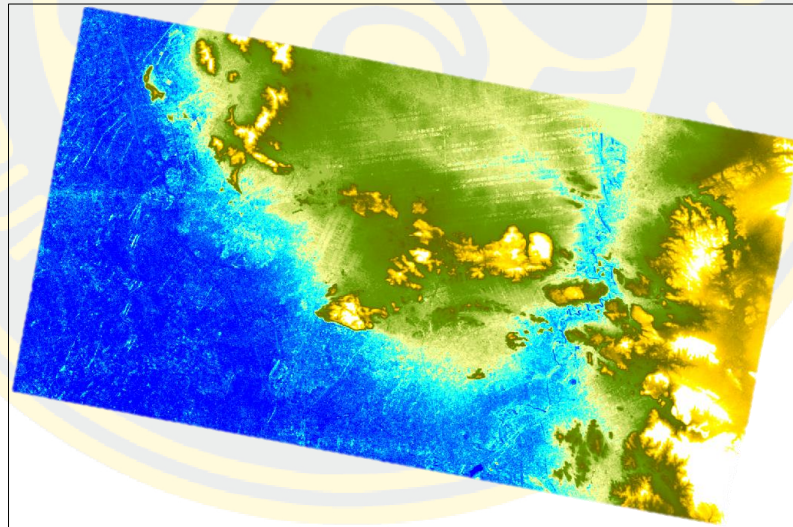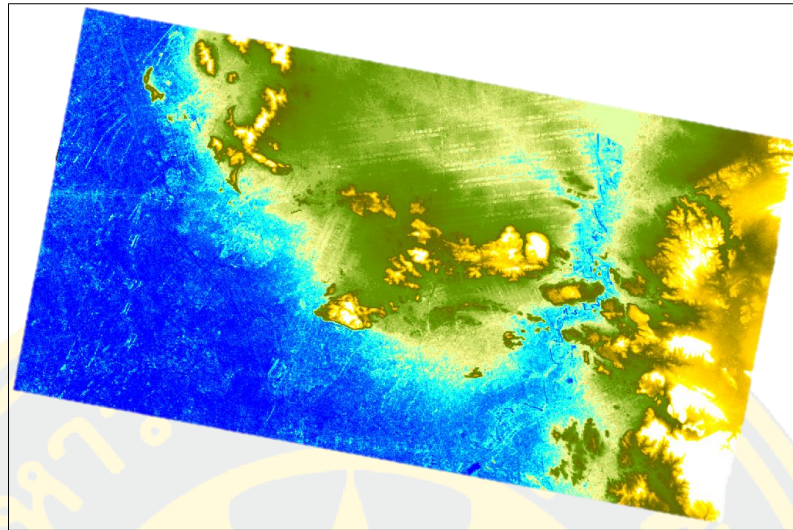

Figure 33 DEM after InSAR process in mining round 1

Figure 34 DEM after InSAR process in mining round 2

4.2.2 Calibration

The DEM result from InSAR process cover both areas of study. Calibration is conducted in total area of study first. Then, divided into each study area. Therefore, consists of 2 results shown in Figure 35 and 37, red area represents the study area. In this process, 506 checkpoints are used for validation. The checkpoints are extracted from RTSD DEM and correct DEM by total area correction by mean difference value from assessment. After process of correction, the R^2 and RMSE in first mining round and second round is obtain as 0.9873, 6.994 m and 0.9865, 7.222 m respectively. As shown the statistic value in Figure 36 and 38.
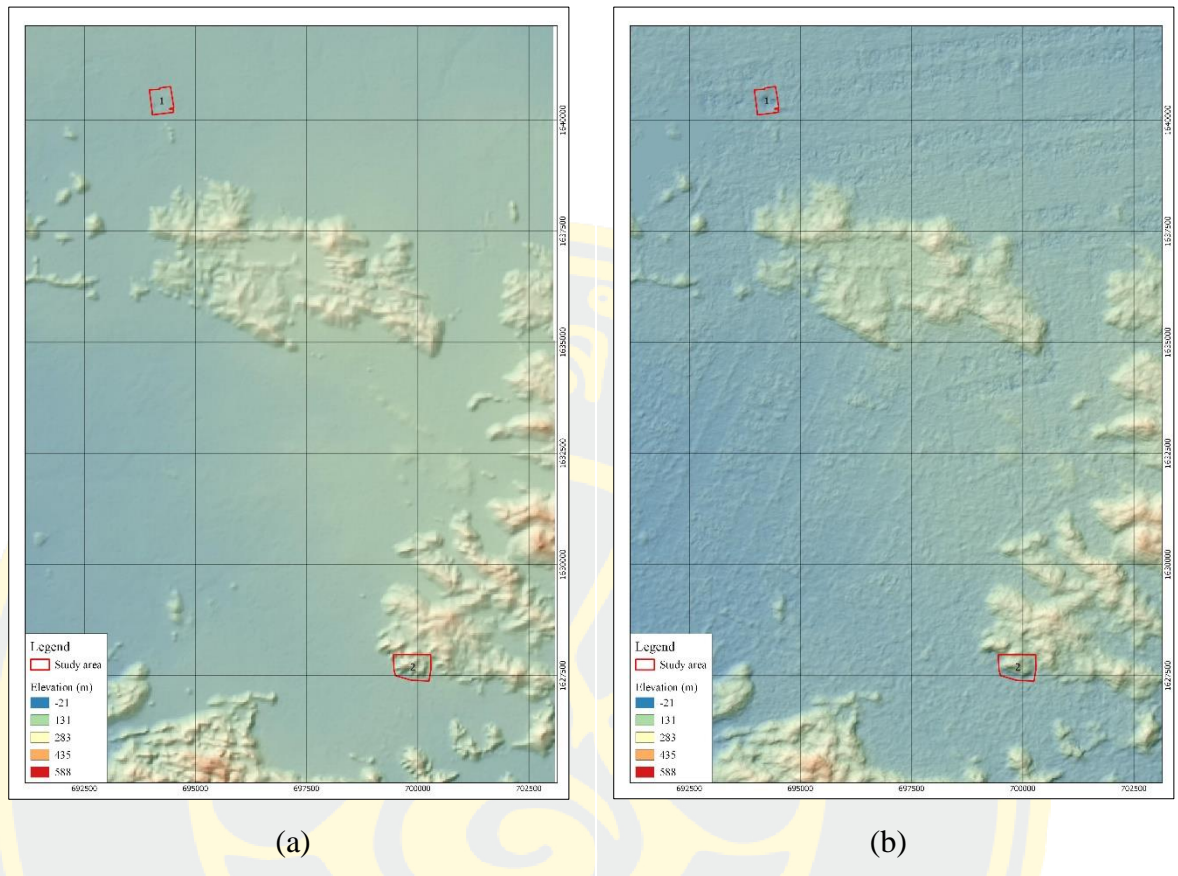
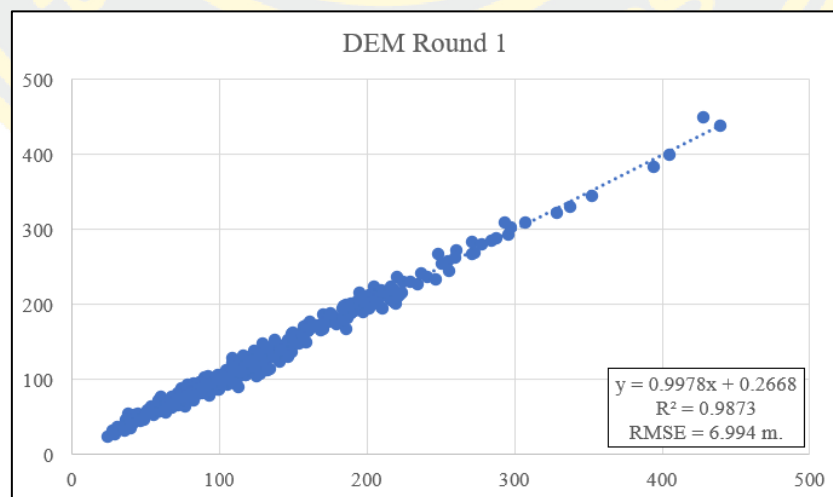**Figure 35** (a) RTSD DEM, (b) DEM from InSAR technique round 1 of mining
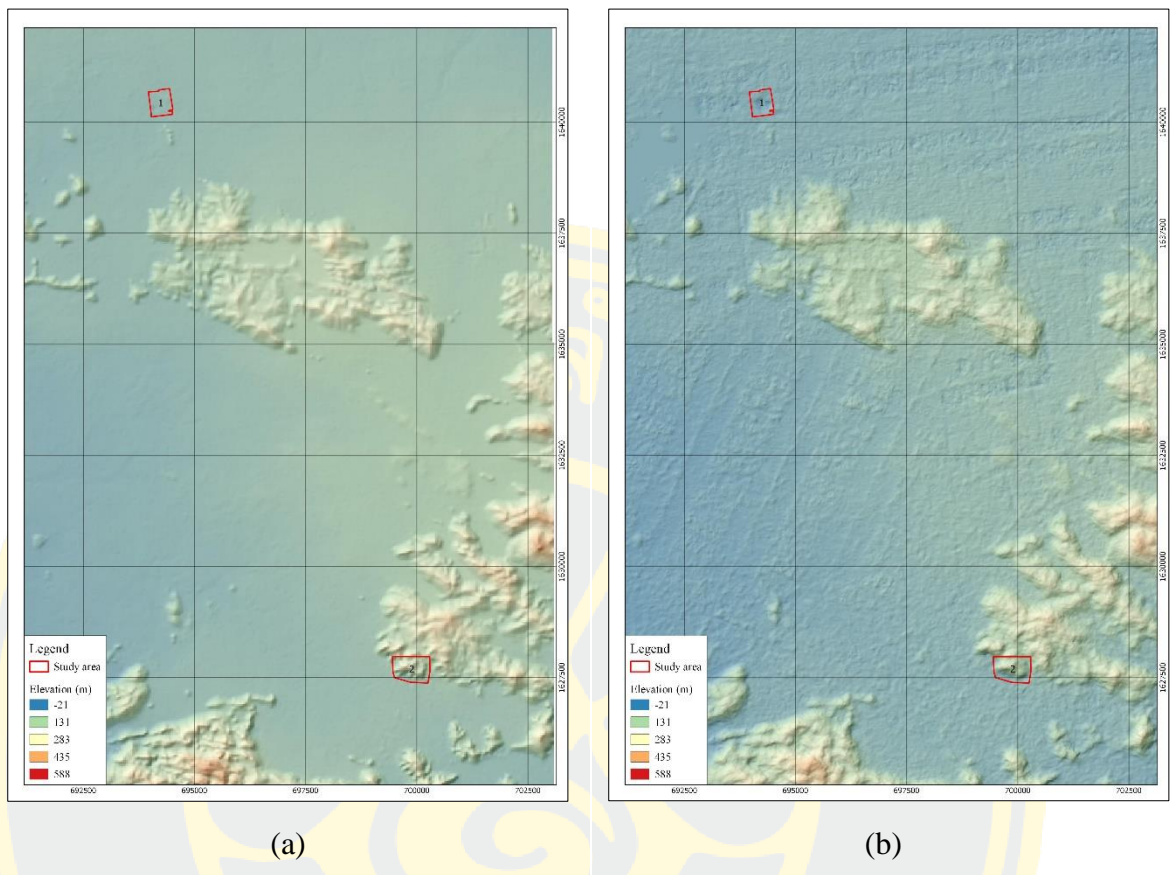

Figure 36 DEM Calibration of round 1 of mining

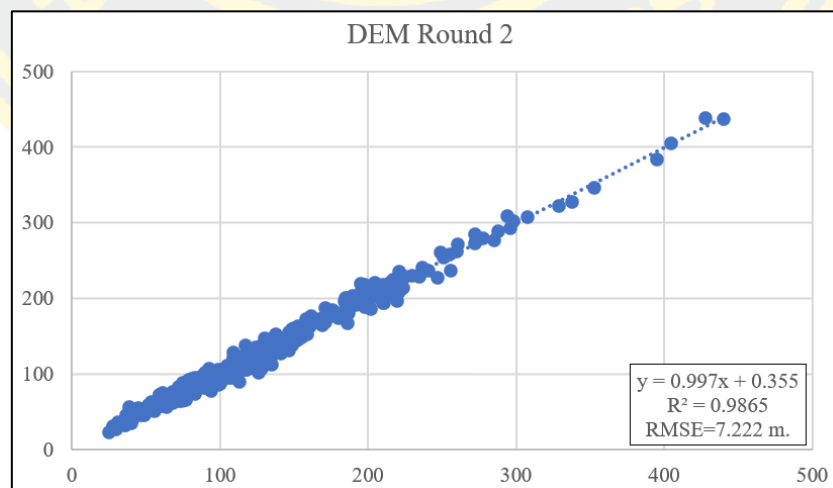**Figure 37** (a) RTSD DEM, (b) DEM from InSAR technique round 2 of mining

Figure 38 DEM Calibration of round 2 of mining

4.2.3 Accuracy Assessment

After the data has been calibrated, it clips specific the study area to validate the data with DEM obtained from the UAV. In each study area, the results were as follows: Study area 1 round 1, DEM result as shown in Figure 39 (a) and the validation results R^2 was 0.6038 and RMSE was 34.279 m, shown in Figure 39 (b). Study area 1 round 2, DEM result as shown in Figure 39 (c) and the validation results R^2 was 0.5621 and RMSE was 35.731 m, shown in Figure 39 (d). Study area 2 round 1, DEM result as shown in Figure 39 (e) and the validation results R^2 was 0.2947 and RMSE was 55.704 m, shown in Figure 39 (f). Study area 2 round 2, DEM result as shown in Figure 39 (g) and the validation results R^2 was 0.2666 and RMSE was 57.603 m, shown in Figure 39 (h).
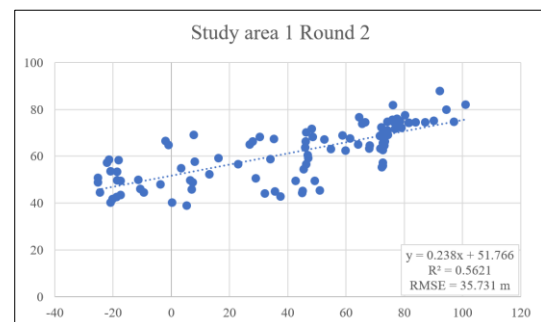

(a)

(b)

(c)

(d)

(e)

(f)

(g)

(h)
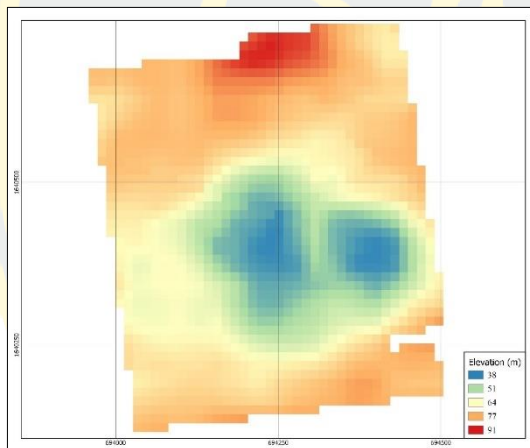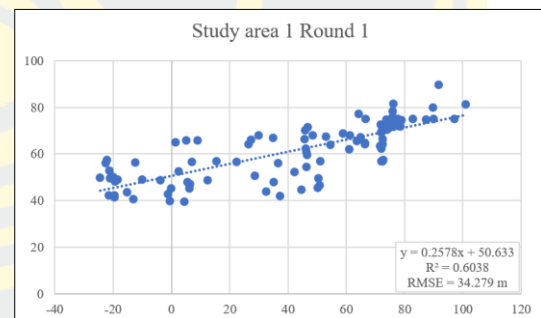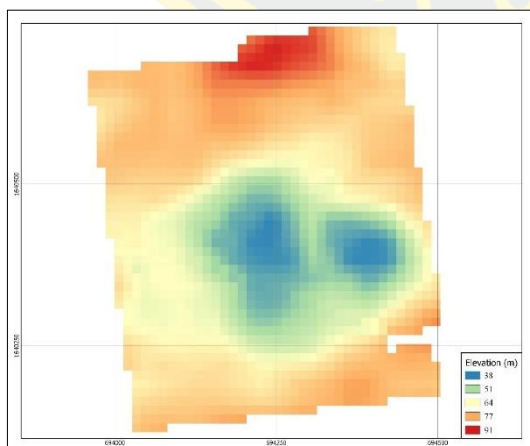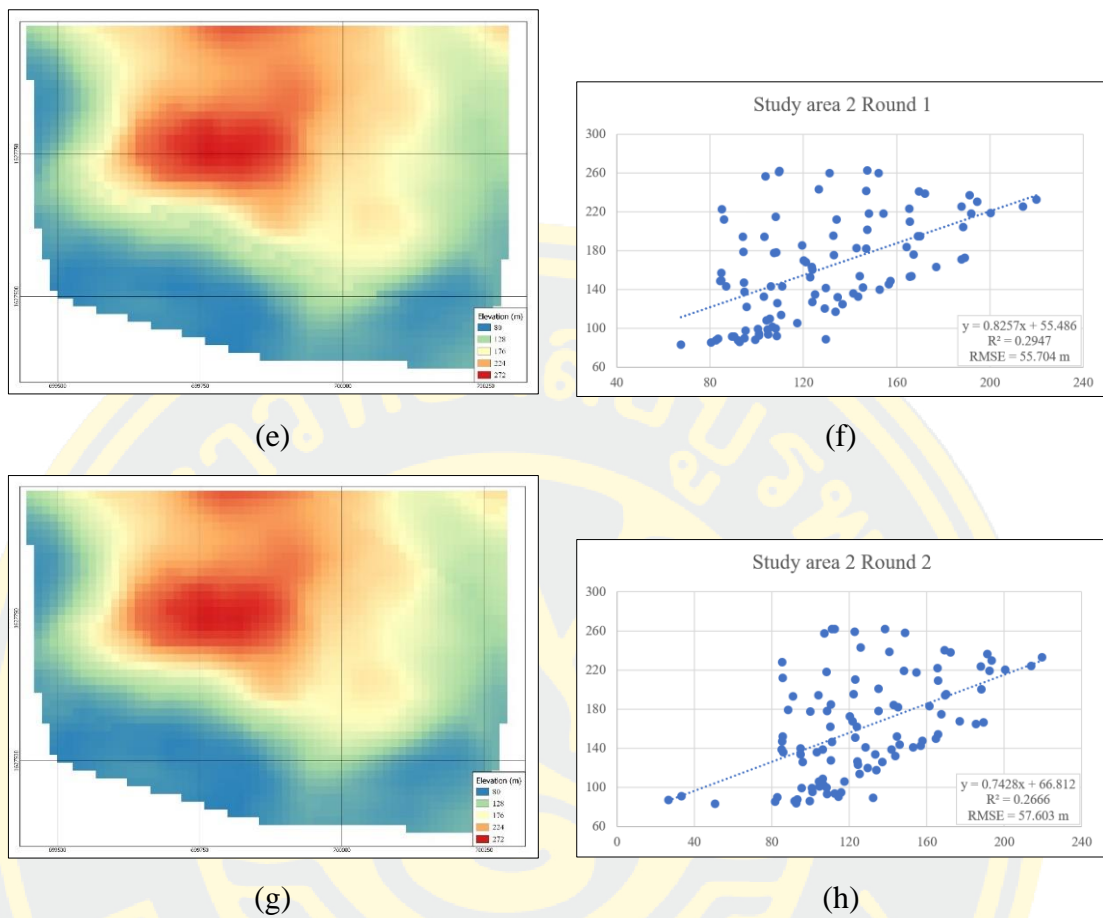
Figure 39 Accuracy results

4.2.4 DEM prepare for vertical change detection

After the DEM validation is complete, they cut off specific mining area based on the boundary of horizontal mining from UAV data for use in analyzing changes in vertical mining boundary. The processing result is DEM with 14 m resolution in each study area details as follows: In study area 1, first mining round has the maximum result of 74.278 m and minimum value is 38.981 m Second mining round obtain 74.463 m and 38.772 m as maximum and minimum value. Whereas, in the study area 2 first mining round has the maximum result of 271.784 m and the minimum value is 92.640 m second mining round obtain maximum and minimum value as 271.342 m and 86.165 m respectively. As shown in Figure 40 to 43.

Figure 40 DEM at the mining site of study area 1 round 1

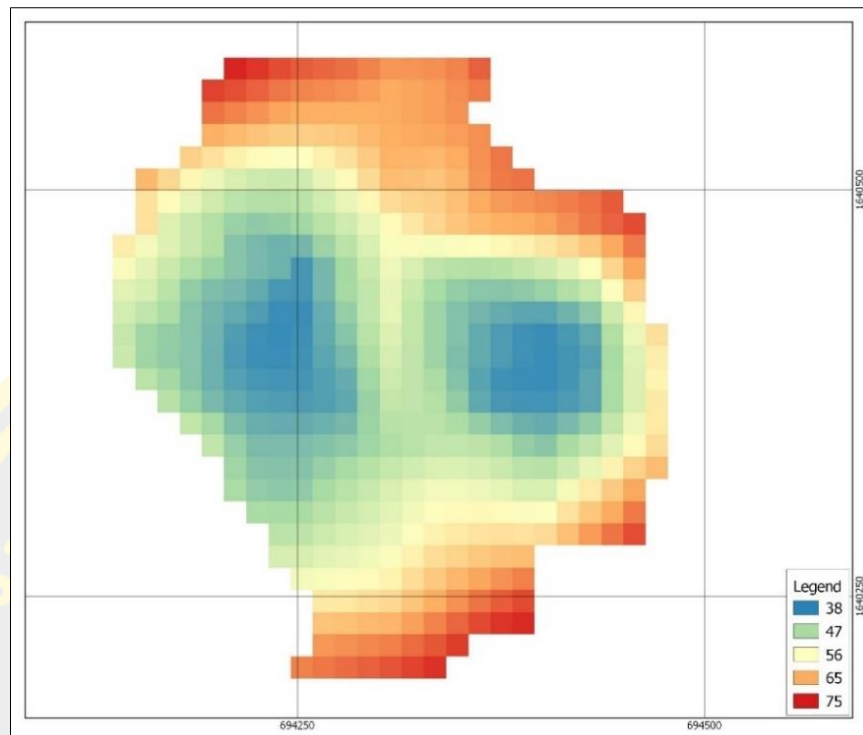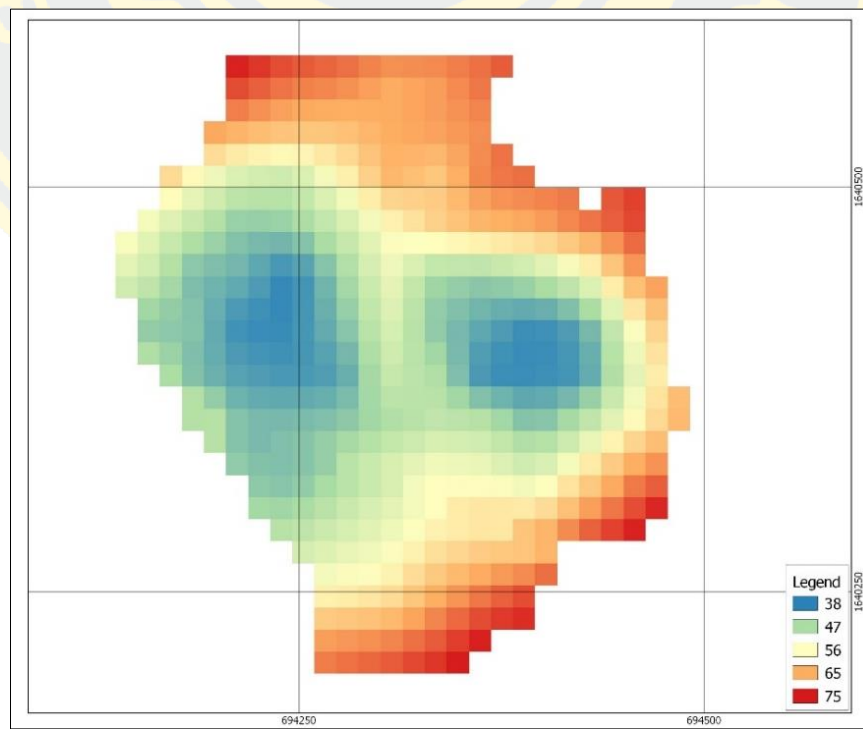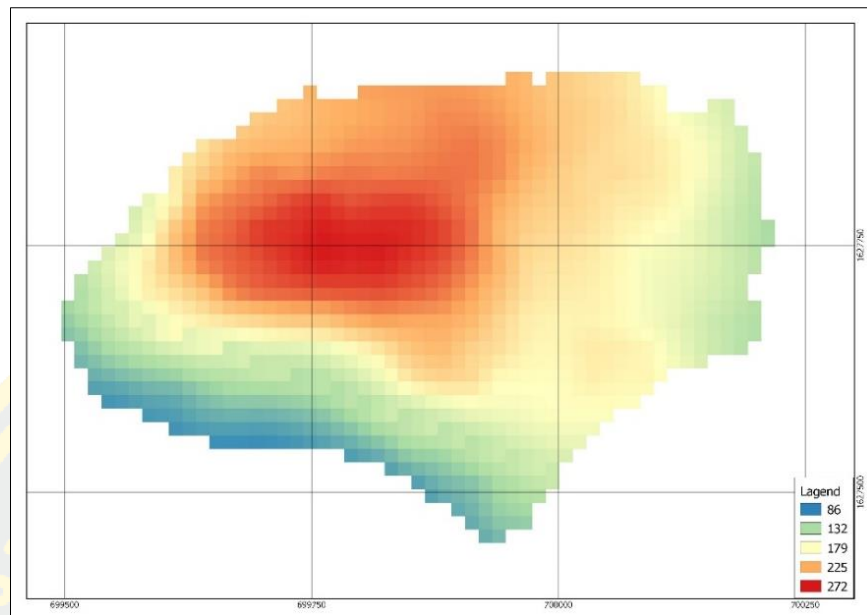**Figure 41** DEM at the mining site of study area 1 round 2

Figure 42 DEM at the mining site of study area 2 round 1
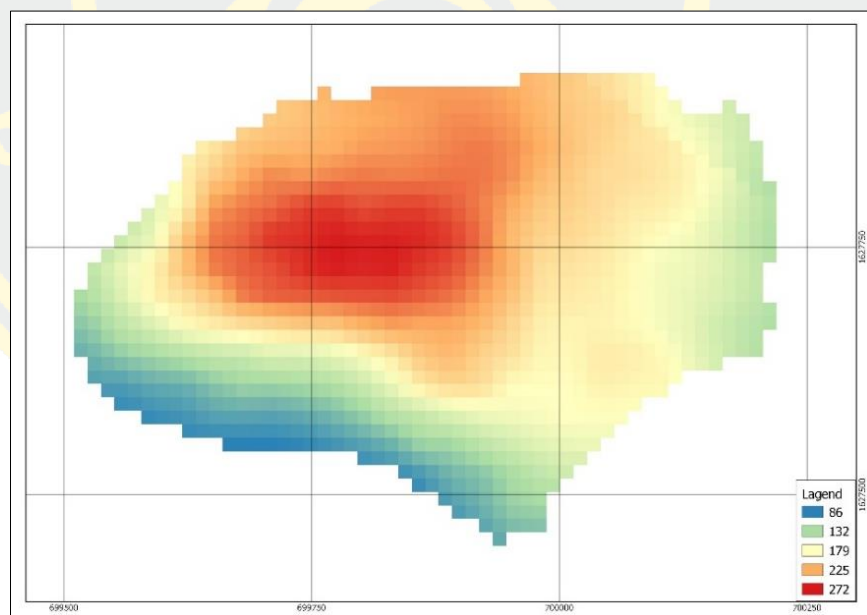
Figure 43 DEM at the mining site of study area 2 round 2

4.3 Change Detection

Change detection of the mining area is including both vertical and horizontal directions. The study results are as follows:

4.3.1 Horizontal Changing

Changes in the mining boundary are shown below and are symbols as follows: red color represents an area that has expanded from mining and green color represents an area that has changed from a mining area to a non-mining area. The result in each study area can be demonstrated as follows.

4.3.1.1 Study area 1

The result of analyzing horizontal change detection in the study area 1 using data from UAV found that there is no change in the mining boundary. The boundary of horizontal mining in the first mining round is shown in Figure 44 (a) and the boundary of horizontal mining in the second mining round is shown in Figure 44 (b). The red line indicates the boundary of horizontal mining whereas the blue line represents the mining area in the study period. As in both figures, mining has occurred only in a vertical direction. There is no change in horizontal expansion during a period of study.

(a)   (b)
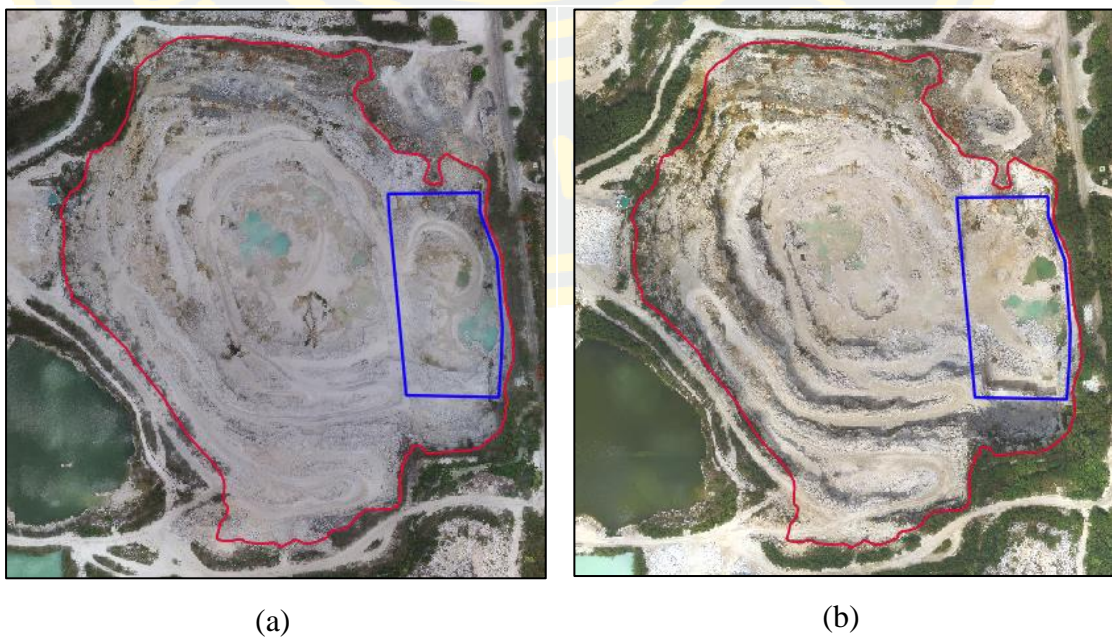
Figure 44 (a) Mining boundary of round 1, (b) Mining boundary of round 2

The analyzing result of the horizontal change in the study area 1 from Sentinel-2 satellite data. The expansion of mining areas is spread around the area. It has a total area of 11,400 m² and the area has changed from a mining area to a non-mining area. It has a total area of 3,300 m². As shown in Figure 45.

Figure 45 Area changed based on Sentinel-2 in study area 1

The analyzing result of the horizontal change in study area 1 from Landsat 8 satellite data reveals that the expansion of the mining area is mainly in the east and west of the area. It has a total area of 19,956 m² and the area has changed from a mining area to a non-mining area. It has a total area of 14,440 m². As shown in Figure 46.

Figure 46 Area changed based on Landsat 8 in study area 1

4.3.1.2 Study area 2

The analyzing result of the horizontal change in study area 2 from UAV data reveals that the expansion of the mining area is mainly in the east of the area. It has a total area of 5,572 m². As shown in Figure 47.

The analyzing result of the horizontal change in study area 1 from Sentinel-2 satellite data reveals that the expansion of mining areas is spread around the area. It has a total area of 26,700 m² and the area has changed from a mining area to a non-mining area. It has a total area of 10,400 m². As shown in Figure 48.
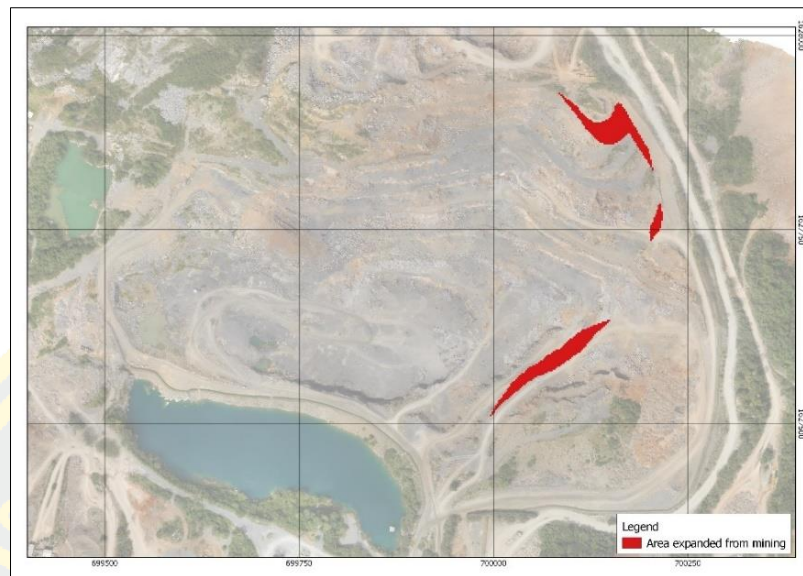
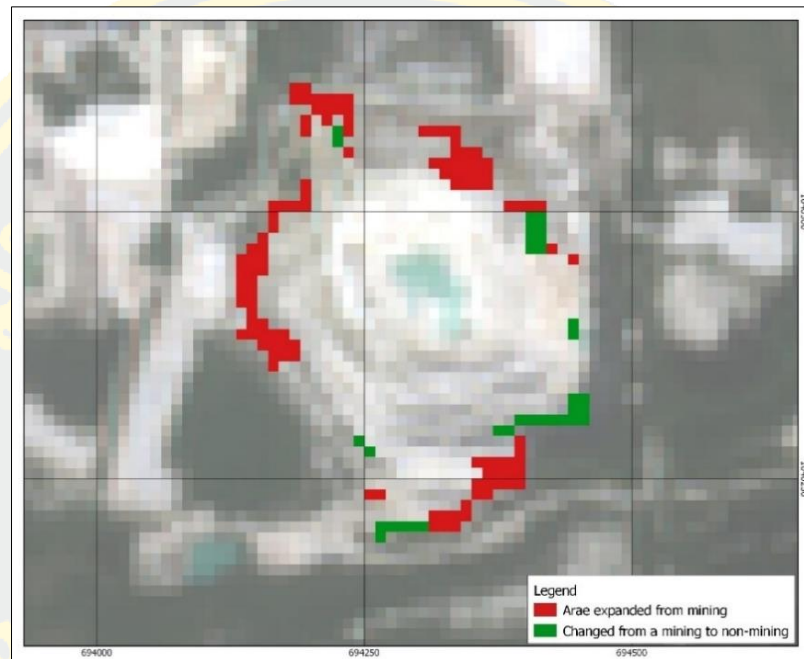**Figure 47** Area changed based on UAV data in study area 2
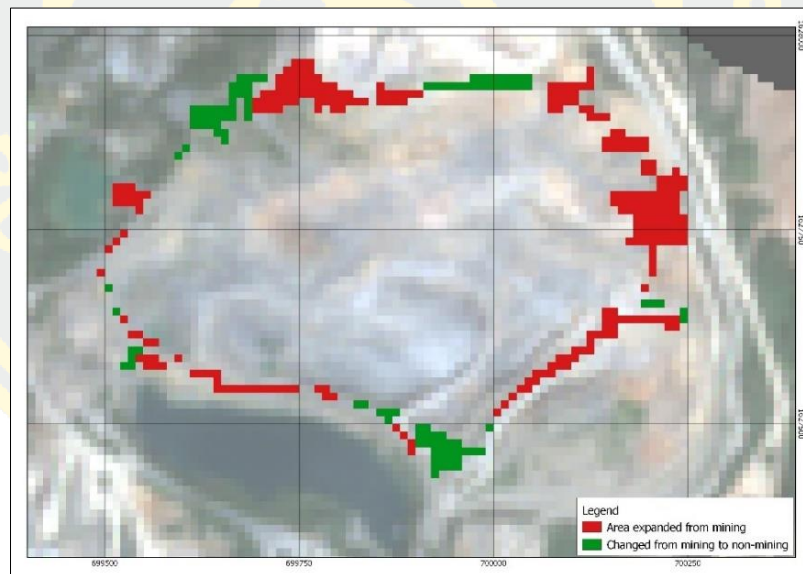
Figure 48 Area changed based on Sentinel-2 in study area 2

The analyzing result of horizontal change in study area 1 from Landsat 8 satellite data reveals that the expansion of the mining area is mainly in the east and west of the area. It has a total area of 31,936 m² and the area has changed from a

mining area to a non-mining area. It has a total area of 26,208 m². As shown in Figure 49.
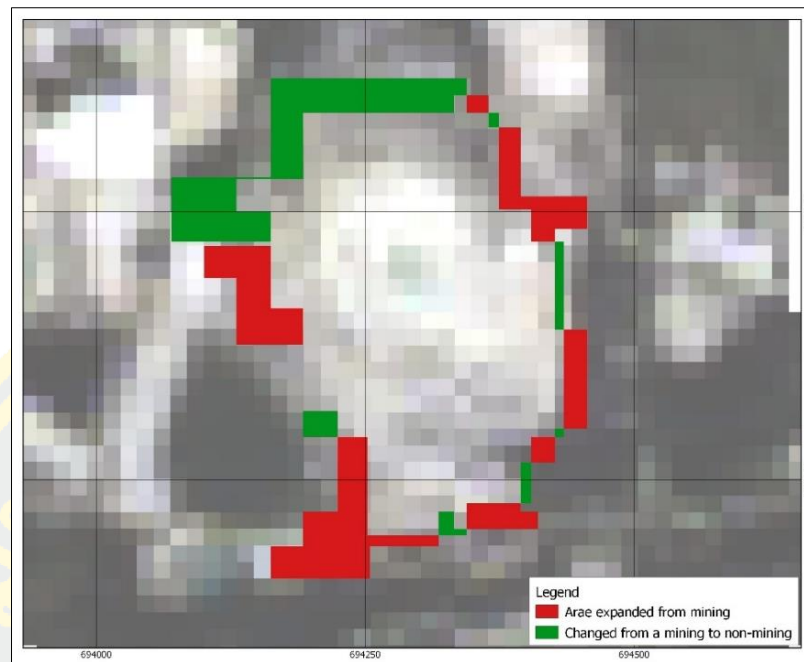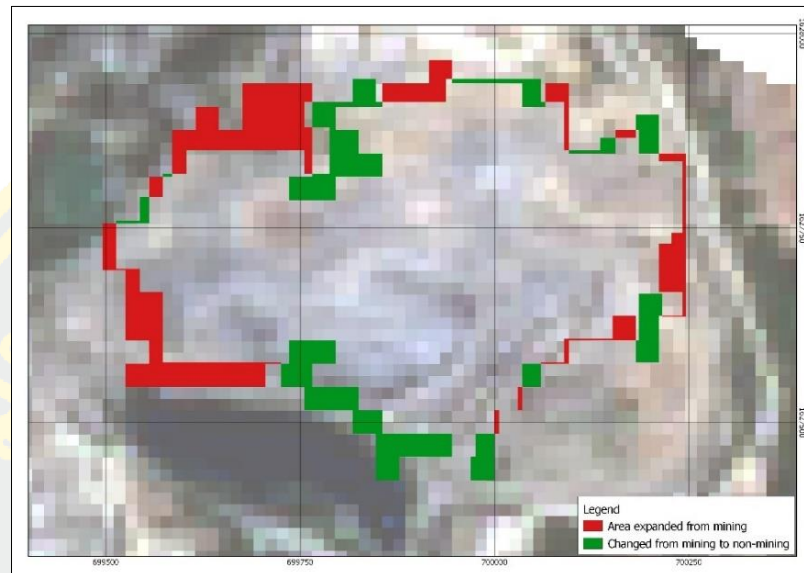

Figure 49 Area changed based on Landsat 8 in study area 2

4.3.2 Vertical Changing

The changing of vertical mining or mining depth is occurred as a consequence of mine digging or from the explosion. Both processes usually happen as normal in the mining area. Mine digging can be conducted in one place and store in another place before transported to production process. The explosion is process which can be obtain massive amount of substance. Therefore, mining volume might be decrease or increase as time changes. The analyzing result of mining volume between 2 periods reveals as follows:

4.3.2.1 Study area 1

The result of calculated volume in the first study area using DEM from UAV found that the cut volume is 141,779.71 m³ and fill volume is 37,743.00 m³. The maximum change is detected in the east of study area (orange area) as shown in Figure 50. This area is characterized by high hill and steep cliff. Mining process is occurring in the period of data collection.
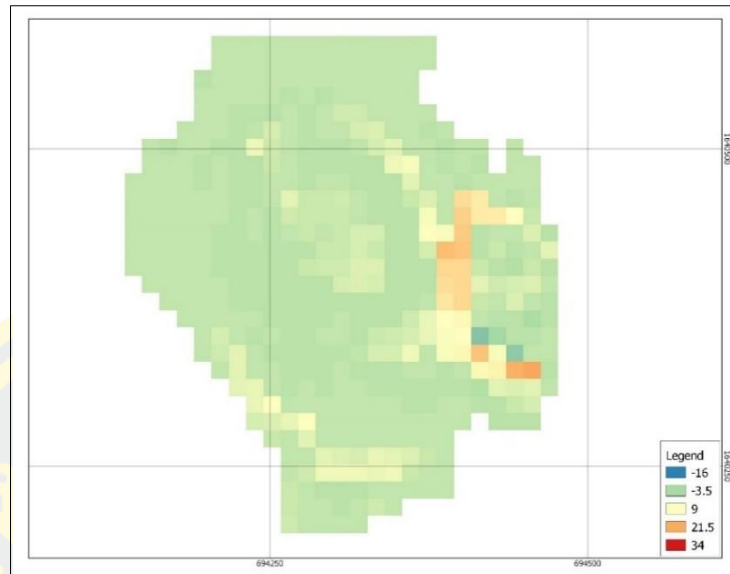
Figure 50 Volume changed based on UAV data in study area 1

The vertical change of mining in study area1 by analyzing DEM from Sentinel-1 found that there is a slightly change of volume. The increasing of volume more than decreasing of mining volume which are fill volume as 69,915.20 m³ and cut volume as 19,945.01 m³ with no correlation with the reference data. Shown in Figure 51.
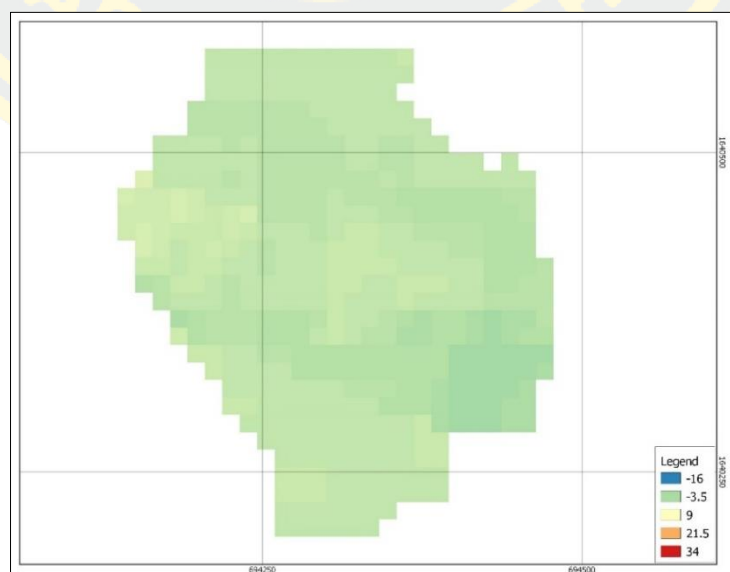
Figure 51 Volume changed based on Sentinel-1 data in study area 1

4.3.2.2 Study area 2

The vertical change of mining in study area 2 by analyzing DEM from UAV found that there is a change throughout the area. This area has large amount of digging process (orange color) indicated the area of decreasing in mining volume. The cut volume is 481,996.86 m³ and fill volume is 79,979.97 m³ (blue color) indicates the area of increasing in volume. As shown in figure 52.

Figure 52 Volume changed based on UAV data in study area 2

The vertical change of mining in study area 2 by analyzing DEM from Sentinel-1 found that the missing volume is occur in the south and west of study area (orange color) with total volume of 635,501.98 m³ and increasing volume is found in center of the area (blue color) is 313,934.75 m³. As shown in Figure 53 with no correlation with the reference data.
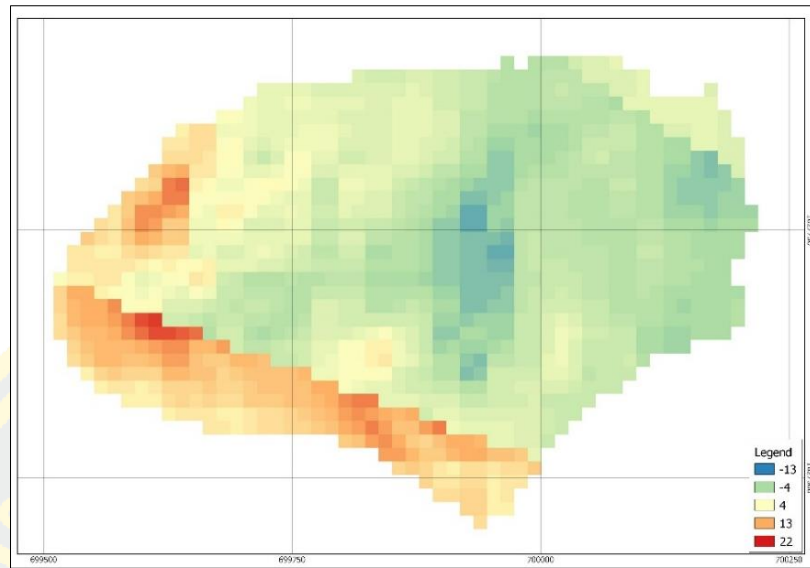
Figure 53 Volume changed based on Sentinel-1 data in study area 2

CHAPTER 5
DISCUSSION AND CONCLUSION

5.1 Discussion

This research detected the change of the boundary of the small mines surface in the horizontal and the vertical directions. The main objectives of the research are applying multi-source satellite imagery to change detection for surface mining boundary, focusing on open-source software in processing. I have extracted the horizontal boundary from the Sentinel-2 and Landsat 8 data using RF algorithm because I try to use 3 algorithms for extraction of horizontal boundary, I found that the RF algorithm is the best accuracy. Then validate using 32 inspection areas in study area 1 and 34 inspection areas in study area 2, the area for validation is selected from UAV data. The overall accuracy was calculated using the confusion matrix in the first study area round 1 which have an overall accuracy of 95.66% and 86.57%. The accuracy of round 2 of the first study area are 97.47% and 96.50%. In the second study area, round 1, the overall accuracy is 100% and 99.35%. For the round 2 of the second study area are 99.26% and 95.90% respectively. As the result, the Sentinel-2 satellite imagery can provide the best accuracy. However, when analyze data above to change detection, the change from satellite data have change from non-mining area to mining area and mining area to non-mining area. In common, changing from mining area to non-mining area is some possible which the reason that stop mining for long time as a result of vegetation cover that area. But this study only the focuses on the expansion of mining due to the main problem of changes in the boundary of mining is the expansion of mines outside the permissible limits.

The results of horizontal change detection show that the Sentinel-2 imagery has a higher agreement with the referent data than Landsat 8 imagery because the Sentinel-2 imagery has a higher resolution than Landsat 8. As a result, extracting the horizontal boundary of mining from its data has higher accuracy as well. However, the results of Sentinel-2 imagery still have a lot of errors compared to the referent data. The area of 97,964.102 m² during the first mining round in study area 1 was used as a reference value for calculating the error from the satellite data. According to the

reference data of change detection result, there is no change of mining in horizontal direction (0% of change comparing to the original area). Meanwhile, the result of Sentinel-2 data found that there is an 11.64 % of change in horizontal mining when compared to the reference data. In the study area2, the mining site covered area of 226,498.761 m² in the first mining round was used as a reference value for calculating the error from satellite data. The change detection result base on reference value found that there is 2% of horizontal expansion compared to the original area. However, the result from Sentinel-2 reveals that there is an 11.79% change in horizontal direction of mining compared to the original area. While analysis of changes in horizontal mining boundary using mining boundary obtained from Landsat 8 in study area 1, mining expansion is 20.37%, and in study area 2, mining expansion is 14.10%.

The extracted DEM from Sentinel-1 with InSAR technique using SNAP Software has 14 m resolution and it had a good correlation when compared to the DEM from RTSD. The correlation value R^2 was 0.987 in the first mining round and 0.987 in the second mining round. However, the RMSE value was 6.994 m in the first mining round and was 7.222 m in the second mining round. Although the DEM data obtained from the InSAR technique has been adjusted, the error values are still high. And when exclude other unrelevent data, the area of study was verified by DEM from UAV, it was found in Study area 1 round 1, R^2 was 0.6038 and RMSE was 34.279 m. Study area 1 round 2, R^2 was 0.5621 and RMSE was 35.731 m. Study area 2 round 1, R^2 was 0.2947 and RMSE was 55.704 m. Study area 2 round 2, R^2 was 0.2666 and RMSE was 57.603 m. This discrepancy has a significant impact on study in small mining areas. Because of the Sentinel-1 data used in this study, each pair of images has very little perpendicular baseline. Consistent with previous research that Sentinel-1 most importantly the length of temporal and perpendicular baselines [26] and they show that the Sentinel-1 mission was mainly designed for the retrieval of deformations (DInSAR) and not good for DEM generation. Therefore, choosing a suitable data to create a DEM would require a perpendicular baseline between 150-300 m long, which in this study, the appropriate data was selected based on a temporal basis with the least value of 12 days, because mining areas are rapidly

changing areas. Therefore, two periods of data must be selected with the least time difference. As a result, it is difficult to choose data with perpendicular baseline as required. It is evident that the results of this study are consistent with the results of a previous study on the efficiency of applying data from Sentinel-1 to generate DEM with the InSAR technique. And in the two study areas, there were different topographic, with study area 1 being flat with less error than the second study area near the mountains, due to the area near the mountains, there is a shadow that obscures the area. This causes processing to be inaccurate, as previous studies have mentioned.

The results of the analysis of volume changes analysis during two periods of mining, focusing on changes that caused vertical mining boundaries to expand or increased mining depth. The results showed that the difference in vertical changes using the DEM from Sentinel-1 and the DEM from UAV in study area 1 was 85.93% and 31.85% in study area 2, respectively. causing the DEM from Sentinel-1 to be relatively low in resolution and high in error, resulting in existence of some errors in detecting the mining changes.

The application of data and methodology in this research is used to detect changes in horizontal and vertical of surface mining boundary. Sentinel-2 has medium level of suitability for change detection of horizontal mining boundary since the change characteristic is near to the reference data. Therefore, it has the potential for the application as a preliminary change detection in order to identify suspected area of mining outside the permissible boundary before the in-situ investigation and surveying. Instead of traditional regulation method of random checking including case of complaint. The adoption of Sentinel-2 images significantly reduces time and cost as well as prevents unnecessary resource loss. On the contrary, the study results suggest that Landsat-8 is not a suitable choice for horizontal change detection in small area mining because the pattern of change did not agree with the reference data. Whereas the vertical change detection of the DEM from Sentinel-1 extracted by InSAR technique found that the Sentinel-1 is not suitable for detect change in vertical mining in small mining area because the difference between it and the reference data

is relatively high. In conclusion, the resolution of the satellite image has significantly affected to the discrepancy value in change detection of small mining areas.

5.2 Conclusion and recommendations

In this research, I have used the Sentinel-2 satellite and Landsat 8 satellite datasets to detect the horizontal boundary change in mining areas. Using QGIS software and two plugins (SCP plugin and Orfeo toolbox). Since the acquiring satellite images, preprocess, extract horizontal boundary of mining, validate, to detect change, I found that the software can download materials faster than downloading from websites as well as processing is also faster. From the materials in this research, I found that the Sentinel-2 had higher accuracy than Landsat 8 in horizontal boundary extraction using Mean-Shift segmentation algorithm and RF algorithm. However, the results are moderately satisfied in change detection compared to reference data from UAV. In conclusion, the satellite image's resolution is directly affecting the correction of analyzed change detection, horizontally. The more limits of mining area it is, the more resolution of satellite image is needed. The InSAR technique to generate the DEM from Sentinel-1 data using SNAP software, which is a tool for processing data from Sentinel satellites, it has good performance in data processing, but requires a highly efficient computer to reduce processing time. Once processed, a DEM is 14 m resolution. Although calibrate has been applied to RTSD DEM but when compared to DEM data from UAV in each area, there are still a lot of differences. And I found the answer about application for horizontal and vertical change detection in the small mining area that Sentinel-2 has medium level of suitability for change detection of horizontal mining boundary since the change characteristic is near to the reference data. While Landsat 8 and Sentinel-1 are low suitability to apply it.

This research has succeeded in goal of applying multi-source satellite imagery to change detection for surface mining boundary, focusing on open-source software in processing. However, if Sentinel-2, Landsat 8, Sentinel-1 data and all method in this study is used for monitoring changes in mining, there will be a great enhancement in the accuracy. therefore, I recommend 1) Higher-resolution satellites should be used to get good results because this study opted for satellite data with free access, which is medium resolution, so the results were not as good as selecting for

high-resolution satellite data, since the resolution of the image point directly affects the accuracy of the result. 2) Choosing a larger study area may make the results more accurate. This study used study area is small size mining because it suits the mining area in Thailand. Using medium-resolution satellite images to analyze change detection in horizontal and vertical mining causes quite a lot of error. 3) Index value of reflection of each type of mineral should be used to help classify the boundary of mining, resulting in better extraction results in the boundary of mining because the different minerals have different reflective values of objects. As a result, classifications using satellite data are also different. 4) Mining data should be selected two periods at least one year apart to make the area change more clearly. Because, this study used two periods of mining data, which had a period of 6 months apart, to analyze changes in mining areas. And in study area 1, there was no change in the horizontal mining area. 5) Reference DEM with a resolution greater than 30 m should be used in the InSAR process to obtain DEM data from sentinel-1 with high accuracy.

REFERENCES

[1]   Dalto, J. (2017). What Is Surface Mining. Retrieved from
        https://www.vectorsolutions.com/resources/blogs/what-is-surface-mining/

[2]   MINERALS ACT,B.E.2560(2017), 134 C.F.R. (2017, 2 March).

[3]   Kotaridis, I. & Lazaridou, M. (2020). Delineation of Open-Pit Mining
        Boundaries on Multispectral Imagery. *Kotaridis, I. and Lazaridou,
        M.(2020). 'Delineation of Open-Pit Mining Boundaries on Multispectral
        Imagery'. in Remote Sensing. IntechOpen. doi, 10*.

[4]   Wang, S. *et al.* (2020). Evaluating the Feasibility of Illegal Open-Pit Mining
        Identification Using Insar Coherence. *Remote Sensing, 12*(3).
        doi:10.3390/rs12030367

[5]   Ibrahim, E., Lema, L., Barnabé, P., Lacroix, P., & Pirard, E. (2020). Small-scale
        surface mining of gold placers: Detection, mapping, and temporal analysis
        through the use of free satellite imagery. *International Journal of Applied Earth
        Observation and Geoinformation, 93*, 102194.
        doi:https://doi.org/10.1016/j.jag.2020.102194

[6]   Wu, Q., Song, C., Liu, K., & Ke, L. (2020). Integration of TanDEM-X and
        SRTM DEMs and Spectral Imagery to Improve the Large-Scale Detection of
        Opencast Mining Areas. *Remote Sensing, 12*(9), 1451. [Online]. Available:
        https://www.mdpi.com/2072-4292/12/9/1451

[7]   Yu, L. *et al.* (2018). Monitoring surface mining belts using multiple remote
        sensing datasets: A global perspective. *Ore Geology Reviews, 101*, 675-687.
        doi:https://doi.org/10.1016/j.oregeorev.2018.08.019

[8]   Resources, D. o. M. (2015). MINERAL RESOURCES OF THAILAND.
        Retrieved from
        http://www.dmr.go.th/main.php?filename=Mineral_re_En#:~:text=A%20numbe
        r%20of%20mineral%20deposits,most%20important%20non%2Dmetallic%20mi
        nerals.

[9]   MCKENZIE, B. (2022). Global Mining Guide - Thailand. Retrieved from
        https://resourcehub.bakermckenzie.com/en/resources/global-mining-guide/asia-
        pacific/thailand/topics/global-mining-guide

[10]   Read, J. M. & Torrado, M. (2009). Remote Sensing. In R. Kitchin & N. Thrift
        (Eds.), *International Encyclopedia of Human Geography* (pp. 335-346). Oxford:
        Elsevier.

[11]   Zhang, Z. & Moore, J. C. (2015). Chapter 4 - Remote Sensing. In Z. Zhang & J.
        C. Moore (Eds.), *Mathematical and Physical Fundamentals of Climate Change*
        (pp. 111-124). Boston: Elsevier.

[12]   Agency, E. S. (2021). Sentinel-2. [Online]. Available:
        https://sentinel.esa.int/web/sentinel/missions/sentinel-2

[13]   Agency, E. S. (2015). Sentinel-2 User Handbook.

[14]   Agency, E. S. (2021). Sentinel-1. Retrieved from
        https://earth.esa.int/web/guest/missions/esa-operational-eo-missions/sentinel-1

[15]   Agency, E. S. (2021). Level-1 SLC Products. Retrieved from
        https://sentinels.copernicus.eu/web/sentinel/technical-guides/sentinel-1-
        sar/products-algorithms/level-1-algorithms/single-look-complex

[16]   Braun, A. (2020). TOPS Interferometry Tutorial for DEM generation.

[17] Lakshmi Narayanan, R. G. & Ibe, O. C. (2015). 6 - Joint Network for Disaster Relief and Search and Rescue Network Operations. In D. Câmara & N. Nikaein (Eds.), *Wireless Public Safety Networks 1* (pp. 163-193): Elsevier.

[18] Agriculture, U. N. I. o. F. a. (2019). GEOSPATIAL TECHNOLOGY. Retrieved from https://mapasyst.extension.org/what-is-an-orthophoto/

[19] Pakoksung, K. & Takagi, M. (2015). Digital elevation models on accuracy validation and bias correction in vertical. *Modeling Earth Systems and Environment, 2*(1), 11. doi:10.1007/s40808-015-0069-3

[20] Balasubramanian, A. (2017). *DIGITAL ELEVATION MODEL (DEM) IN GIS*.

[21] Team, N. M. A. J. S. a. U. S. J. A. S. (2019). ASTER Global Digital Elevation Model V003 [Data set]. Retrieved from https://doi.org/10.5067/ASTER/ASTGTM.003

[22] Dempsey, C. (2019). Version 3 of the ASTER Global Digital Elevation Model Released. Retrieved from https://www.gislounge.com/version-3-of-aster-global-digital-elevation-model-released/

[23] Survey, U. S. G. (2021). InSAR-Satellite-based technique. [Online]. Available: https://www.usgs.gov/natural-hazards/volcano-hazards/insar-satellite-based-technique-captures-overall-deformation-picture

[24] Alganci, U., Besol, B., & Sertel, E. (2018). Accuracy Assessment of Different Digital Surface Models. *ISPRS International Journal of Geo-Information, 7*(3). doi:10.3390/ijgi7030114

[25] Zhou, H., Zhang, J., Gong, L., & Shang, X. (2012). Comparison and Validation of Different DEM Data Derived from InSAR. *Procedia Environmental Sciences, 12*, 590-597. doi:10.1016/j.proenv.2012.01.322

[26] Braun, A. (2021). Retrieval of digital elevation models from Sentinel-1 radar data – open applications, techniques, and limitations. *Open Geosciences, 13*(1), 532-569. doi:doi:10.1515/geo-2020-0246

[27] Organization), G.-I. a. S. T. D. A. P. (2013). *Fundamental Geographic Data Set: FGDS*.

[28] Mondini, A. C., Santangelo, M., Rocchetti, M., Rossetto, E., Manconi, A., & Monserrat, O. (2019). Sentinel-1 SAR Amplitude Imagery for Rapid Landslide Detection. *Remote Sensing, 11*(7). doi:10.3390/rs11070760

[29] Agency, E. S. SNAP. Retrieved from https://earth.esa.int/eogateway/tools/snap

[30] Ponguta, S. Global mapper. Retrieved from https://www.geoilenergy.com/en/software/geosoluciones/global-mapper

[31] Jangid, A. (2017). *Introduction to QGIS*.

[32] Toolbox, O. (2019). Open Source processing of remote sensing images Retrieved from https://www.orfeo-toolbox.org/

[33] QGIS. (2020). A Free and Open Source Geographic Information System. Retrieved from https://qgis.org/en/site/

[34] Congedo, L. (2021). Semi-Automatic Classification Plugin: A Python tool for the download and processing of remote sensing images in QGIS. *Journal of Open Source Software, 6(64)*.

[35] Detection, R. S. f. F. C. C. (2016). Module 3: Introduction to QGIS and Land Cover Classification. Retrieved from https://servirglobal.net/Portals/0/Documents/Articles/ChangeDetectionTraining/Module3_LC_Classification_Accuracy_Assessment.pdf

[36] Huang F, C. Y., Li L, Zhou J, Tao J, Tan X, et al. (2019). Implementation of the parallel mean shift-based image segmentation algorithm on a GPU cluster. *International Journal of Digital Earth, 12(3):328-53.*

[37] Michel J, Y. D., Grizonnet M. (2015). Stable Mean-Shift Algorithm and Its Application to the Segmentation of Arbitrarily Large Remote Sensing Images. *IEEE Trans Geosci Remote Sensing, 53(2):952-64.*

[38] Berhane, T. M. *et al.* (2018). Decision-Tree, Rule-Based, and Random Forest Classification of High-Resolution Multispectral Imagery for Wetland Mapping and Inventory. *Remote Sensing, 10*(4). doi:10.3390/rs10040580

[39] Volke, M. I. & Abarca-Del-Rio, R. (2020). Comparison of machine learning classification algorithms for land cover change in a coastal area affected by the 2010 Earthquake and Tsunami in Chile. *Nat. Hazards Earth Syst. Sci. Discuss., 2020*, 1-14. doi:10.5194/nhess-2020-41

[40] Scherer, J. A. *Comparison of the Practical Applications and Limitations of InSAR and Structure From Motion Depictions of Surface Elevation Flux for Academic Purposes.* (Undergraduate Honors Thesis). Available from CU Boulder CU Scholar database.

[41] To, S. H. (2021). RMSE: Root Mean Square Error. [Online]. Available: https://www.statisticshowto.com/probability-and-statistics/regression-analysis/rmse-root-mean-square-error/

[42] Chicco D, W. M., Jurman G. (2021). The coefficient of determination R-squared is more informative than SMAPE, MAE, MAPE, MSE and RMSE in regression analysis evaluation. *PeerJ Computer Science 7:e623*, 18.

[43] Bock, T. What is R-Squared. Retrieved from https://www.displayr.com/what-is-r-squared/

APPENDIX

APPENDIX A. Quality Report of UAV data

1. Quality Report of orthophoto and DEM data from DPIM in study area 1 round 1.

Figure A.1 Quality Report of study area 1 round 1

2. Quality Report of orthophoto and DEM data from DPIM in study area 1 round 2.

Figure A.2 Quality Report of study area 1 round 2

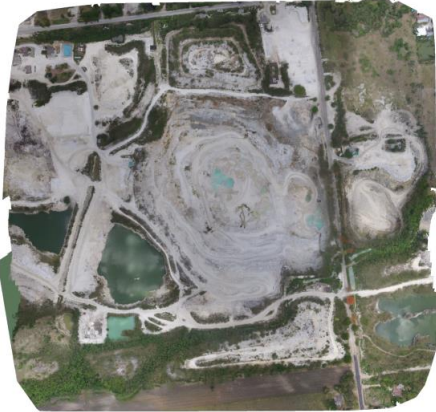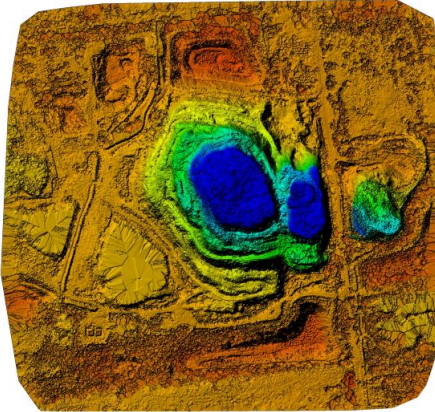3. Quality Report of orthophoto and DEM data from DPIM in study area 2 round 1.

Figure 1: Orthomosaic and the corresponding sparse Digital Surface Model (DSM) before densification.

Figure A.3 Quality Report of study area 2 round 1

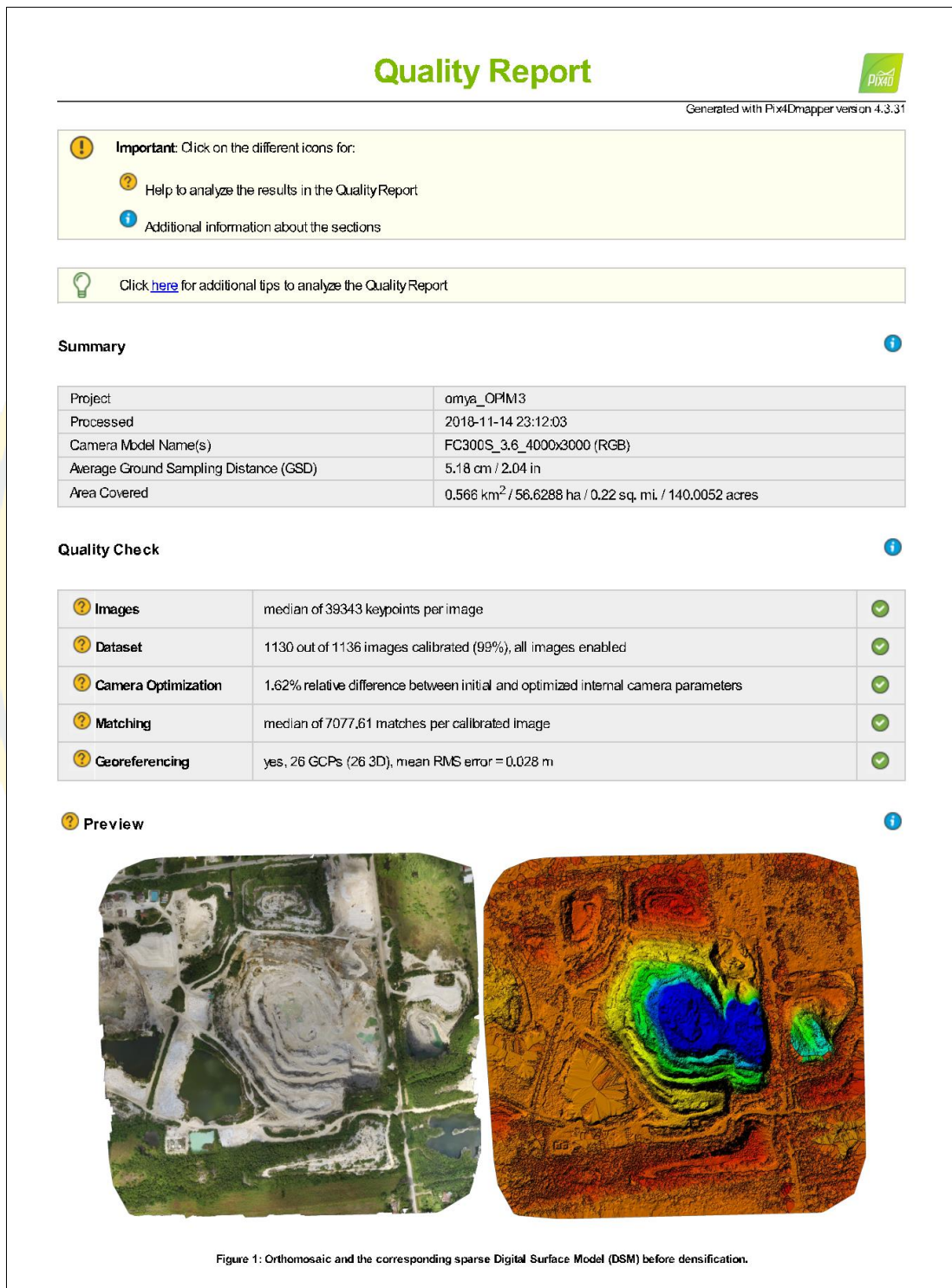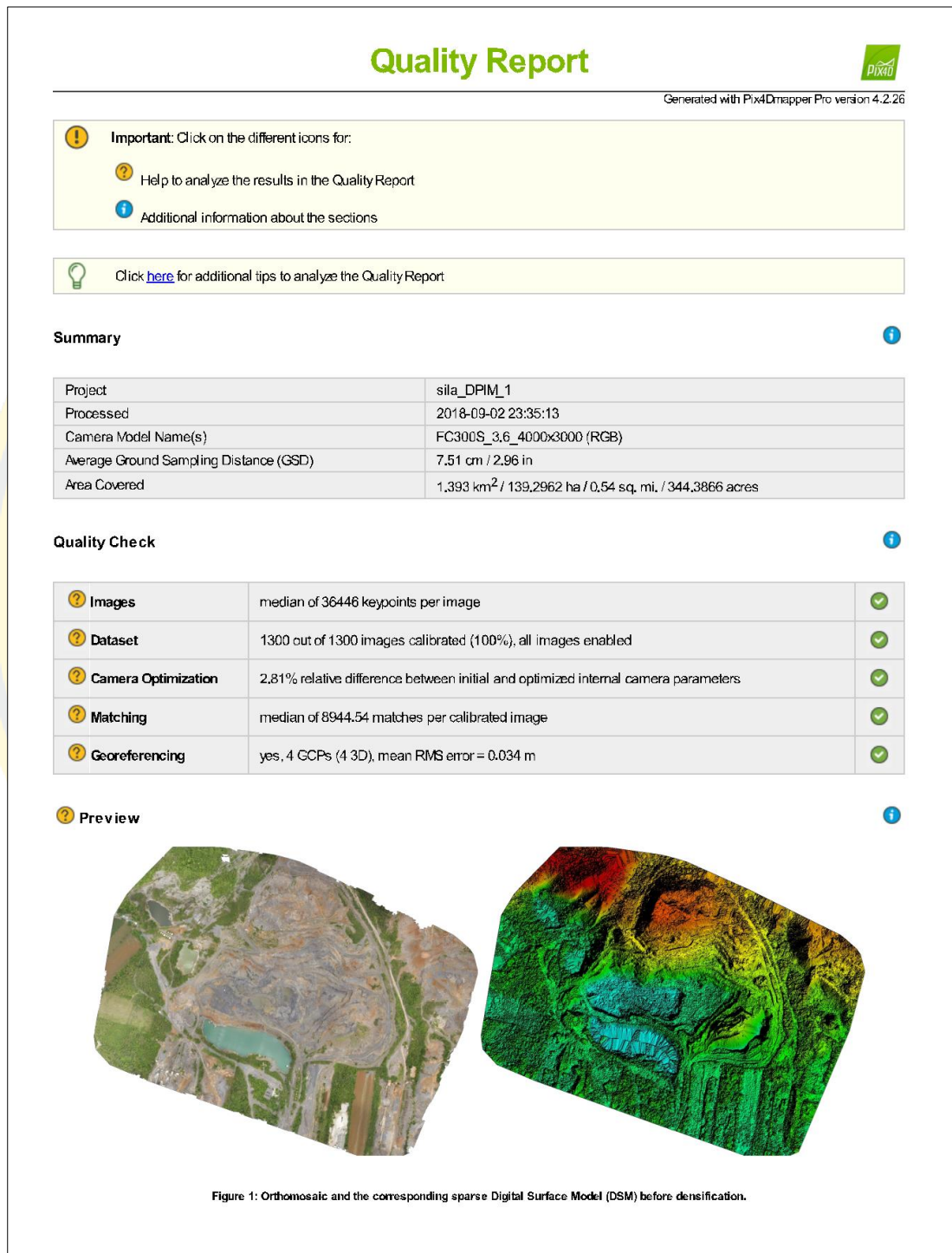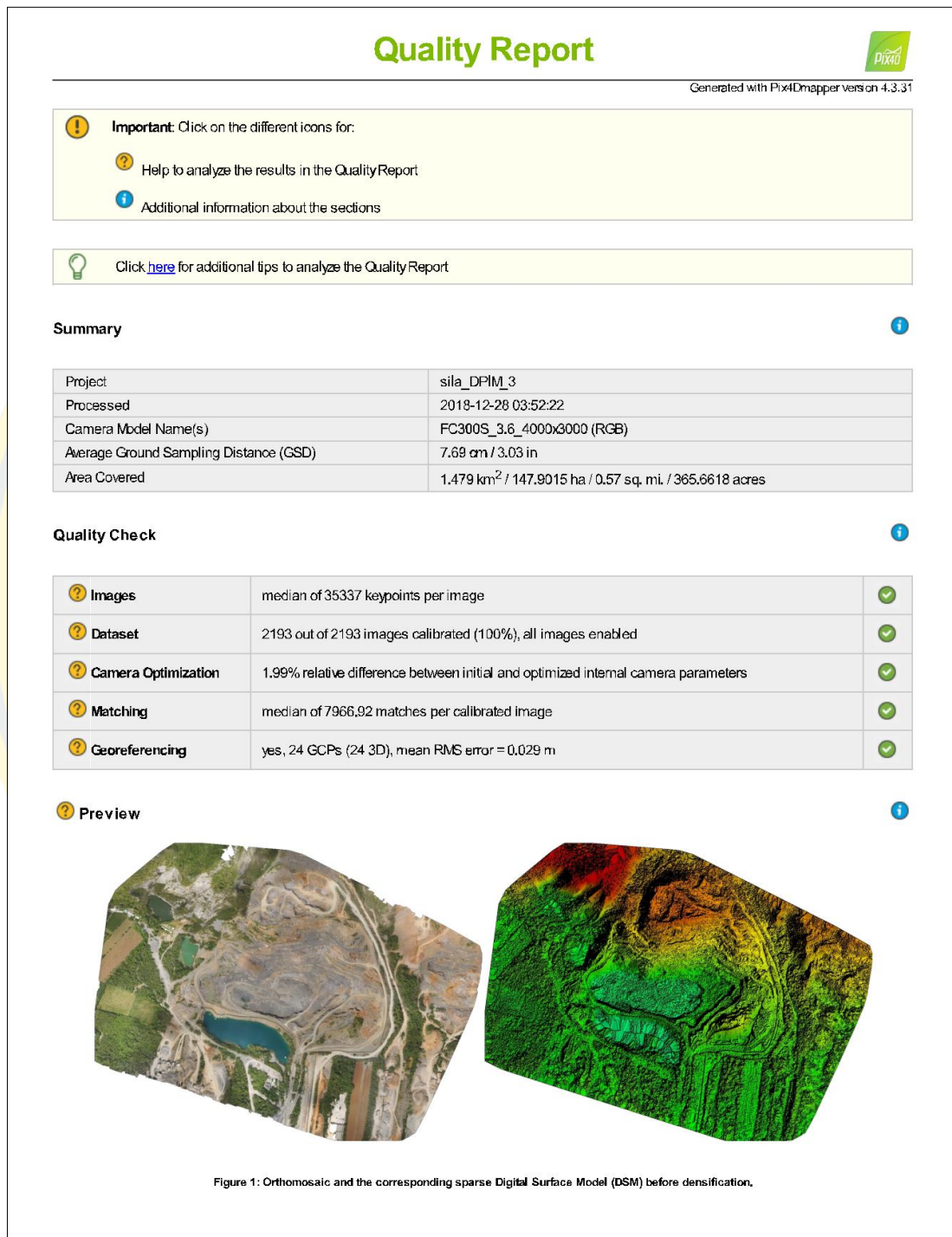4. Quality Report of orthophoto and DEM data from DPIM in study area 2 round 2.

Figure A.4 Quality Report of study area 2 round 2

APPENDIX B. Classification of horizontal mining boundaries

Extraction of the horizontal boundary, the training area is defined from UAV Orthophoto divided into five class: Mining, Bare soil, Road, Water, and Vegetation for classifying satellite imagery and the red line represents the mining boundary as a reference.
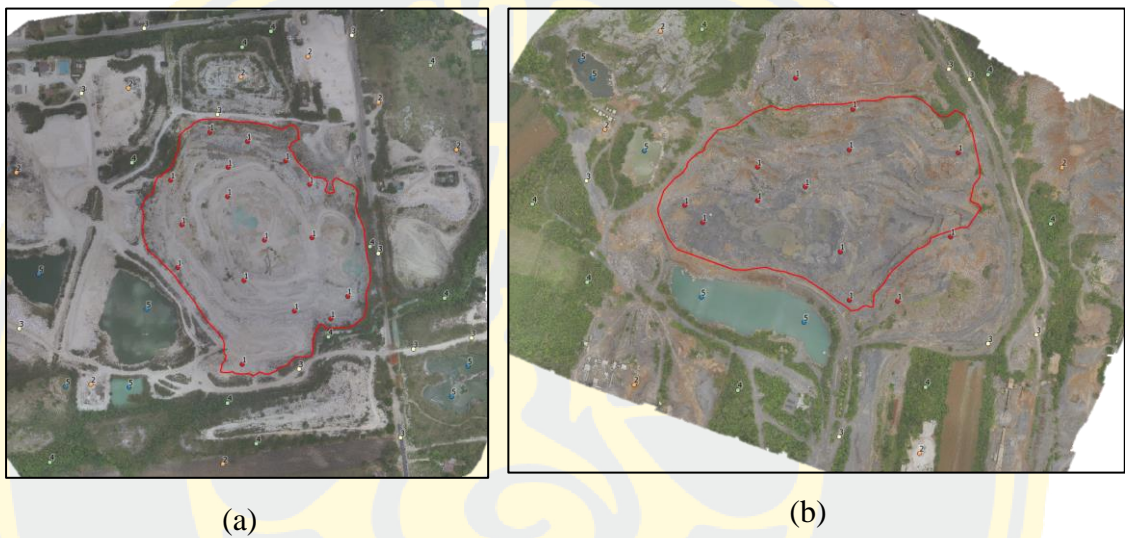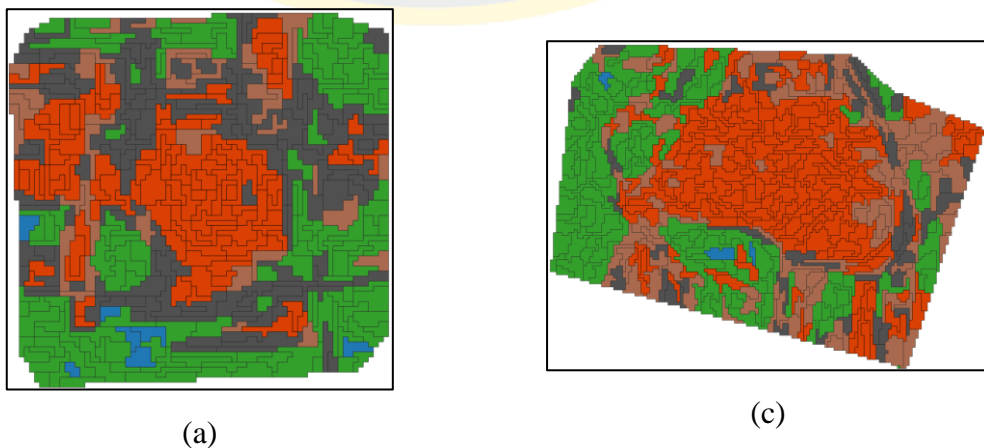

(a)

(b)

Figure A.5 Training point, (a) Study area 1, (b) Study area 2

The result of the horizontal boundary extraction, segmented with mean-shift algorithms, then Classify with Random Forest algorithms will get land cover into 5 classes. Extraction from Sentinel-2 show in figure A.6, A.6 (a and b) represent to study area 1, A.6 (c and d) represent to study area 2.
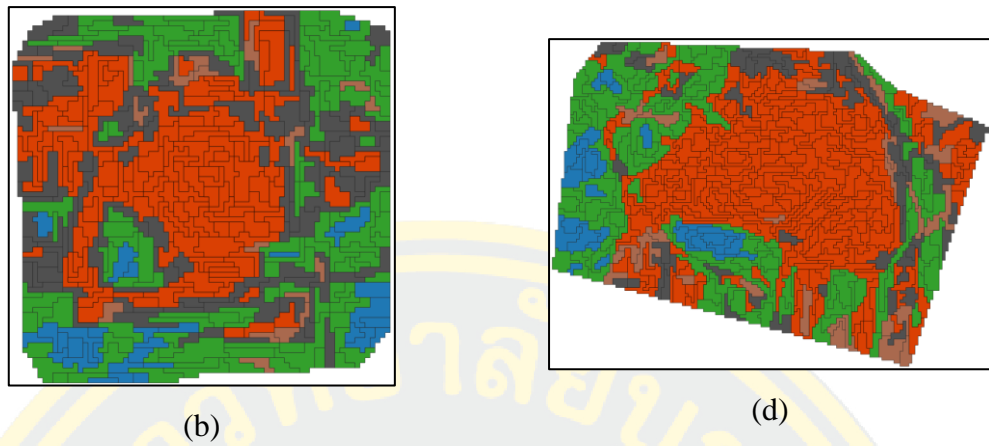

(a)

(c)

(b)

(d)

Figure A.6 Classification result from Sentinel-2

And from Landsat 8 show in Figure A.7, A.7 (a and b) represent to study area 1, A.7 (c and d) represent to study area 2.

(a)

(c)

(b)

(d)
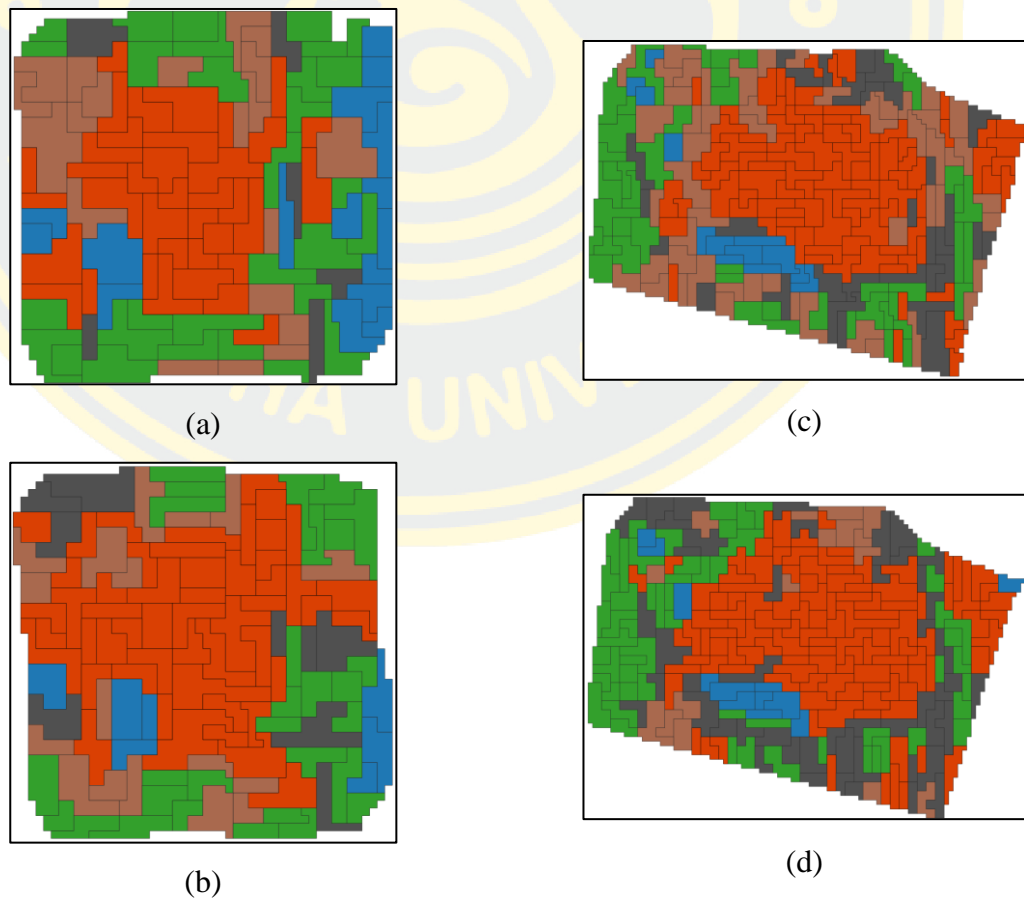
Figure A.7 Classification result from Landsat 8

APPENDIX C. Data for validation of horizontal mining boundaries

Figure A.8 Testing area for study area 1

Red polygons refer to mining class and green polygons refer to non-mining class.

Table A.1: Detail of testing area of study area 1

No.	ClassID	Class Type	Coordinates (m)	
			Northing	Easting
1	1	Mining	1,640,448.02	694,336.64
2	1	Mining	1,640,498.93	694,436.63
3	1	Mining	1,640,585.32	694,217.83
4	1	Mining	1,640,432.74	694,149.20

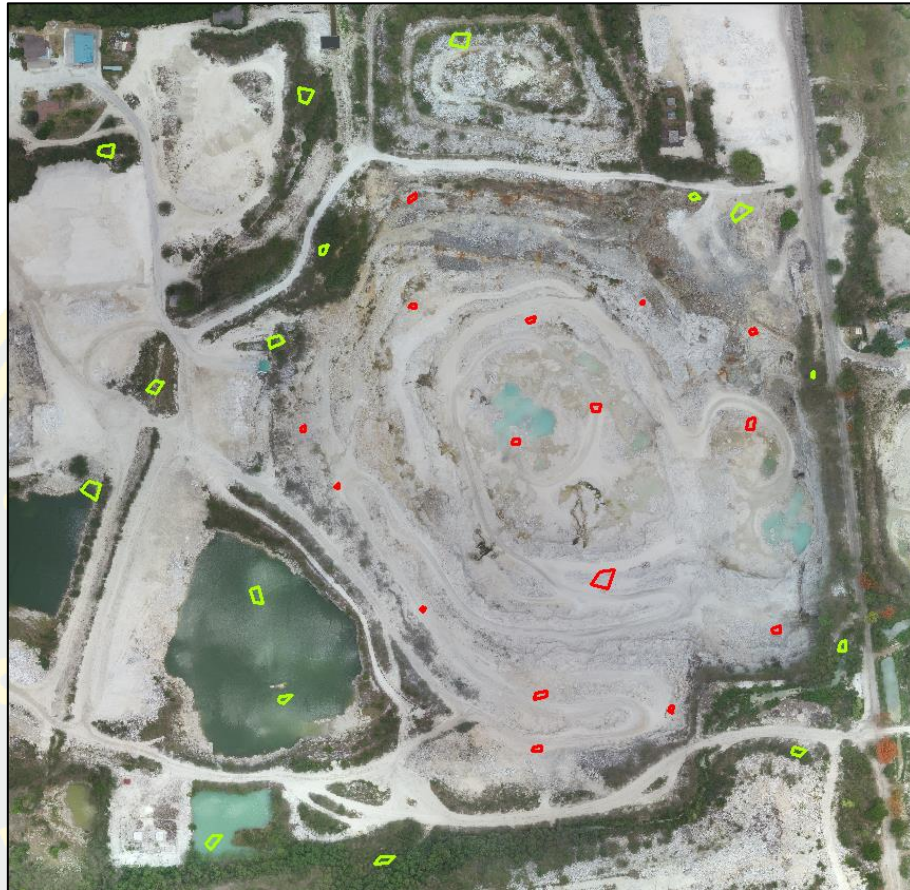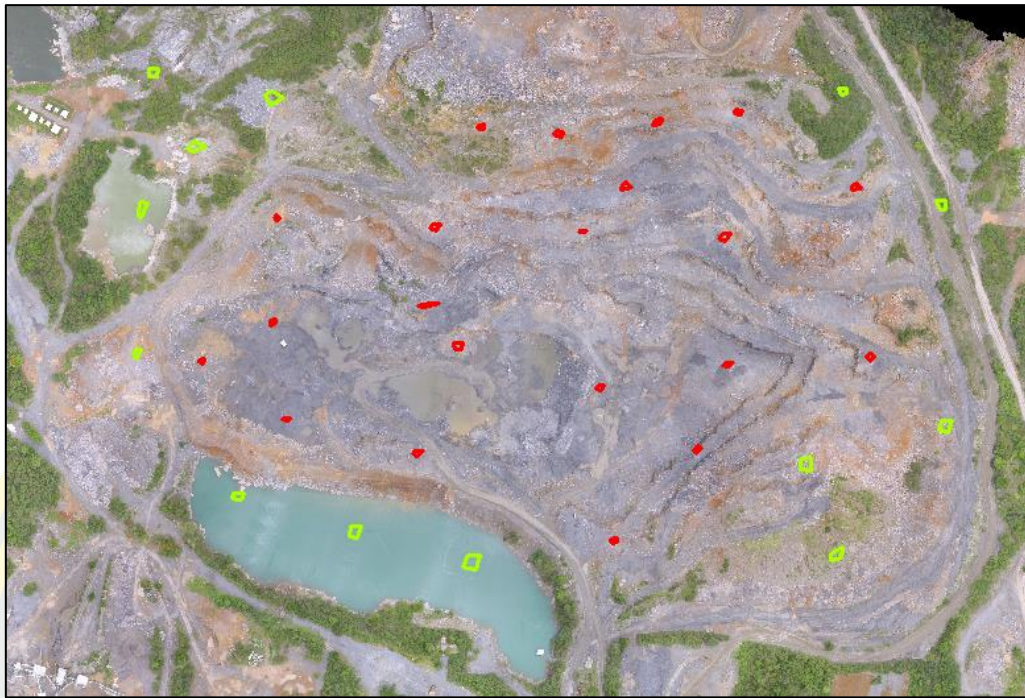| No.	ClassID	Class Type	Coordinates (m)	
			Northing	Easting
5	1	Mining	1,640,258.55	694,302.79
6	1	Mining	1,640,223.19	694,300.77
7	1	Mining	1,640,302.75	694,453.44
8	1	Mining	1,640,335.23	694,342.39
9	1	Mining	1,640,438.23	694,435.87
10	1	Mining	1,640,514.28	694,219.00
11	1	Mining	1,640,425.35	694,285.76
12	1	Mining	1,640,314.57	694,226.86
13	1	Mining	1,640,517.50	694,365.72
14	1	Mining	1,640,249.97	694,386.38
15	1	Mining	1,640,395.14	694,171.36
16	1	Mining	1,640,505.40	694,294.59
17	2	Non-Mining	1,640,322.62	694,120.14
18	2	Non-Mining	1,640,550.76	694,161.08
19	2	Non-Mining	1,640,587.64	694,398.44
20	2	Non-Mining	1,640,292.23	694,495.72
21	2	Non-Mining	1,640,222.67	694,467.63
22	2	Non-Mining	1,640,149.25	694,203.74
23	2	Non-Mining	1,640,160.58	694,093.70
24	2	Non-Mining	1,640,459.57	694,054.29
25	2	Non-Mining	1,640,652.51	694,148.85
26	2	Non-Mining	1,640,689.47	694,247.89
27	2	Non-Mining	1,640,577.77	694,428.23
28	2	Non-Mining	1,640,490.05	694,130.83
29	2	Non-Mining	1,640,614.95	694,021.73
30	2	Non-Mining	1,640,471.09	694,475.44
31	2	Non-Mining	1,640,391.56	694,014.22
32	2	Non-Mining	1,640,254.71	694,138.66

Figure A.9 Testing area for study area 1

Red polygons refer to mining class and green polygons refer to non-mining class.

Table A.2: Detail of testing area of study area 2

| ID | ClassID | Class Type | Coordinates (m) | |
			Northing	Easting
1	1	Mining	1,627,662.01	700,187.94
2	1	Mining	1,627,476.85	699,940.82
3	1	Mining	1,627,562.47	699,749.26
4	1	Mining	1,627,595.04	699,621.35
5	1	Mining	1,627,652.47	699,538.51
6	1	Mining	1,627,795.77	699,610.64
7	1	Mining	1,627,788.51	699,764.17
8	1	Mining	1,627,882.46	699,883.64
9	1	Mining	1,627,905.55	700,057.99

ID	ClassID	Class Type	Coordinates (m)	
			Northing	Easting
10	1	Mining	1,627,831.64	700,173.26
11	1	Mining	1,627,780.87	700,045.72
12	1	Mining	1,627,784.94	699,907.67
13	1	Mining	1,627,629.39	699,925.95
14	1	Mining	1,627,653.62	700,049.73
15	1	Mining	1,627,710.16	699,757.20
16	1	Mining	1,627,670.06	699,787.58
17	1	Mining	1,627,691.91	699,607.17
18	1	Mining	1,627,830.87	699,948.79
19	1	Mining	1,627,888.44	699,808.22
20	1	Mining	1,627,568.14	700,021.10
21	1	Mining	1,627,894.98	699,979.88
22	2	Non-Mining	1,627,916.18	699,605.91
23	2	Non-Mining	1,627,927.03	700,159.94
24	2	Non-Mining	1,627,814.48	700,256.33
25	2	Non-Mining	1,627,594.16	700,261.49
26	2	Non-Mining	1,627,464.07	700,157.57
27	2	Non-Mining	1,627,454.42	699,802.67
28	2	Non-Mining	1,627,517.99	699,574.70
29	2	Non-Mining	1,627,803.89	699,479.82
30	2	Non-Mining	1,627,940.56	699,489.21
31	2	Non-Mining	1,627,554.37	700,126.23
32	2	Non-Mining	1,627,483.62	699,688.77
33	2	Non-Mining	1,627,866.77	699,530.54
34	2	Non-Mining	1,627,660.15	699,475.47

APPENDIX D. Data for validation of DEM from Sentinel-1

To process the accuracy assessment, I used 100 random checkpoints in each area, covering all elevation ranges, show in Figure:
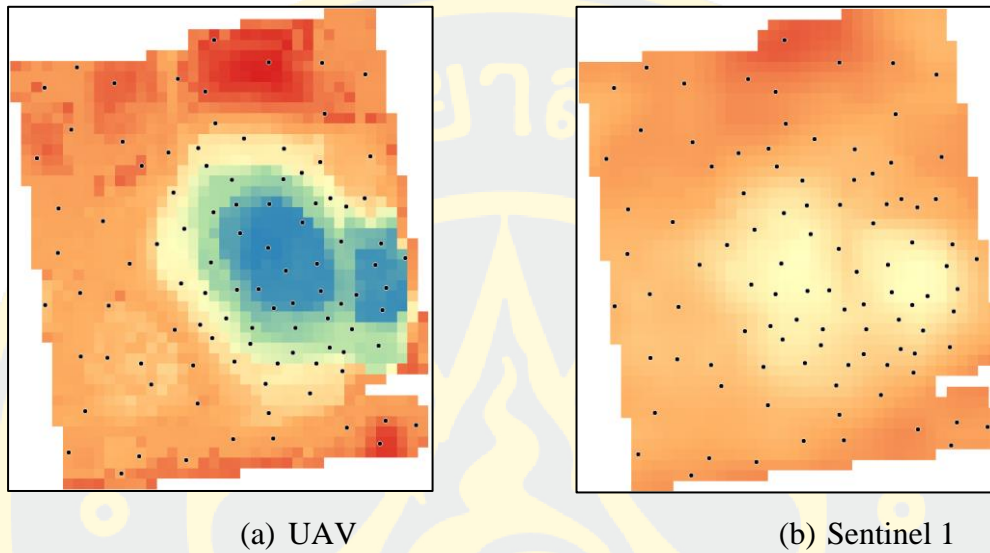

(a) UAV   (b) Sentinel 1

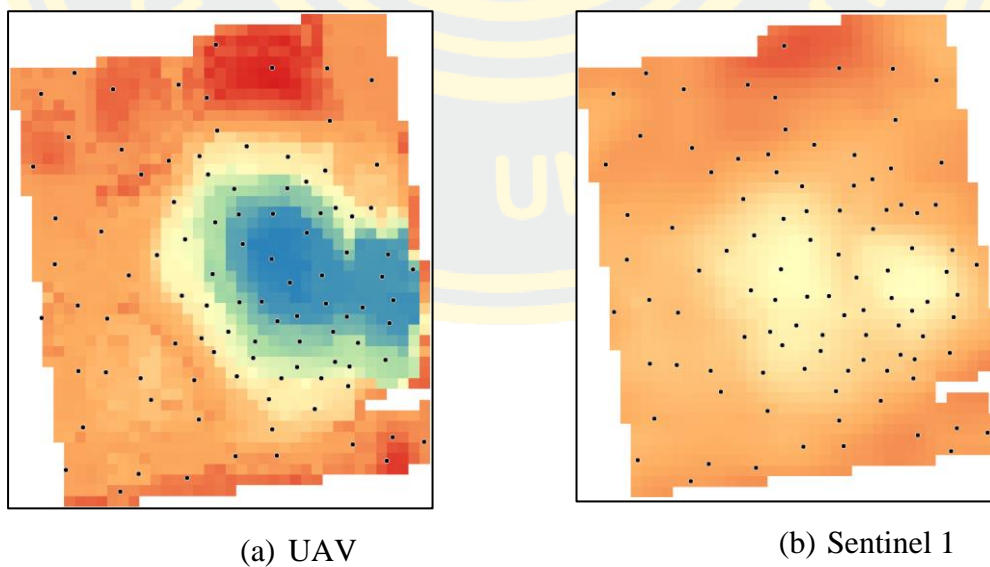**Figure A.10** Accuracy assessment of study area 1 round 1

(a) UAV   (b) Sentinel 1

Figure A.11 Accuracy assessment of study area 1 round 2

(a) UAV   (b) Sentinel 1
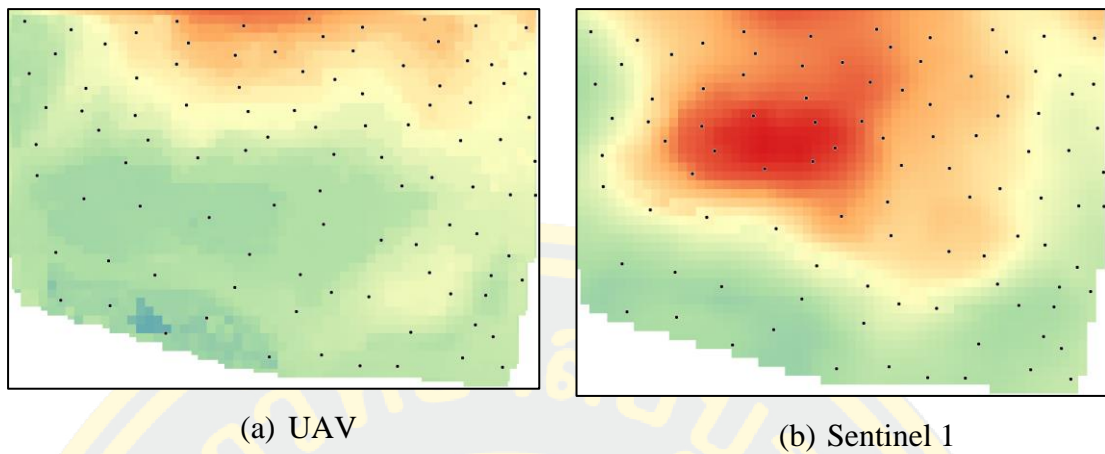
Figure A.12 Accuracy assessment of study area 2 round 1

(a) UAV   (b) Sentinel 1
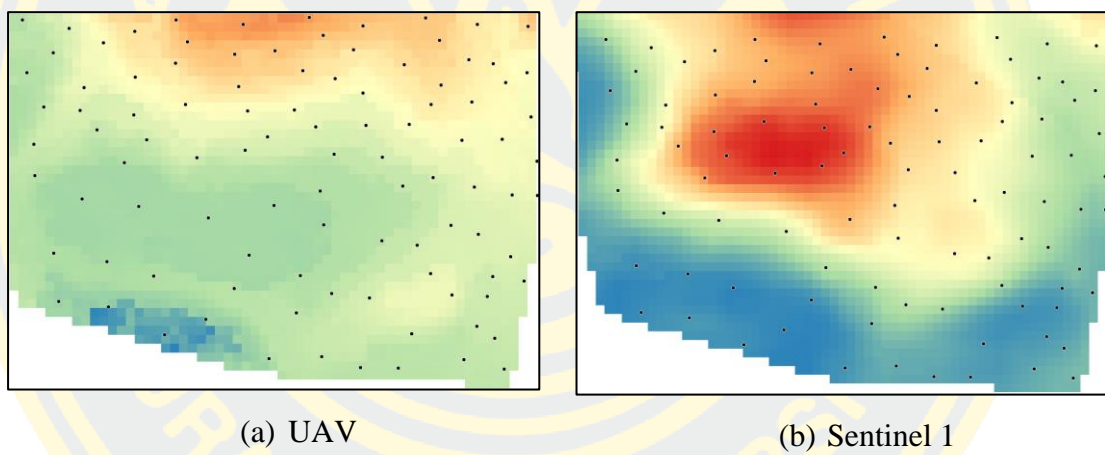
Figure A.13 Accuracy assessment of study area 2 round 2

BIOGRAPHY

NAME	Kawipa Sukkee
DATE OF BIRTH	29 March 1995
PLACE OF BIRTH	Songkhla
PRESENT ADDRESS	953 Talad Sub-district, Phra Pradaeng District, Samut Prakan, 10130
POSITION HELD	Survey engineer at Department of Primary Industries and Mines.
EDUCATION	Bachelor of Engineering (Survey Engineering) for First-Class Honours, Rajamangala University of Technology Srivijaya.